IJISET - International Journal of Innovative Science, Engineering & Technology, Vol. 6 Issue 6, June 2019
ISSN (Online) 2348 – 7968
www.ijiset.com

Investigation of Mechanical and Thermal Properties of Drum Brake For Light Duty Vehicle Application

Brhan Dinberu[1], Maj. Dr. Bisrat Yoseph[2]

[1] P.G. Student Department of Mechanical Engineering, Addis Ababa Science and Technology, Addis Ababa, Ethiopia
brhandinberu@gmail.com

[2] Associate Professor Department Of Motor Vehicle Engineering, Bisfoftu Defense Engineering, Bishoftu, Ethiopia
ethiobisrat@gmail.com

Abstract

This thesis deals with Investigation of Mechanical and Thermal Properties of Drum Brake for Light Duty Vehicle Application. Brakes of an automobile generally fail when the working stress exceeds the maximum permissible stress and excessive heating of brake drum. During the application of shoe force gives rise to the mechanical loads. in this study to analyze the mechanical and thermal properties of drum brake and friction plate for light duty vehicle application numerically using SOLID WORK premium 2016 and ANSYS WORKBENCH. And experimentally analysis the wear and hardness properties of three commercial friction plate as compare to the local products. Using JF160 chasese taster and Rockwell hardness tester. The fade and recovery of friction plates reading shows the quality of imported products is not good as compare to the local products. The strength and the heat dissipation of finned drum brake is better than normal (flat) drum brakes.

Keywords: *SOLIDWORK, ANSYS WORKBENCH, Brake drum, Fin, wear & hardness*

1. Introduction

Drum brakes were the first types of brakes used on motor vehicles. Nowadays, over 100 years after the first usage, drum brakes are still used on the rear wheels of most vehicles. The drum brake is used widely as the rear brake particularly for small car and motorcycle. The leading-trailing shoe design is used extensively as rear brake on passenger cars and light weight pickup trucks. Most of the front-wheel-drive vehicles use rear leading-trailing shoe brakes. Such design provided low sensitivity to lining friction changes and has stable torque production (Limpert, 1999).

Drum brake is composed of mobile and immobile elements. Immobile elements are via backing plate (1) attached to the supporting structure of the vehicle, while moving parts (drum (2)) are connected to wheel hub. Friction elements of drum brakes are two symmetrically placed brake shoes and drum. During brake activation, brake shoes snuggle up with the drum and thus the car's kinetic energy is converted into heat, i.e. braking of the vehicle is performed. Drum brakes' shoes are composed of a metal carrier part (3) and friction lining (4). The connection between the metal part and friction lining can be achieved by riveting (rivets (5)), bonding (only by glue or by glue and a chemical process during vulcanization), or by a combination of these two methods, depending on the brake's type. Brake shoes of simplex brakes are supported at lower ends, and in particular, at drum brakes shown in Fig.1, on clamping of the brake adjuster (6).

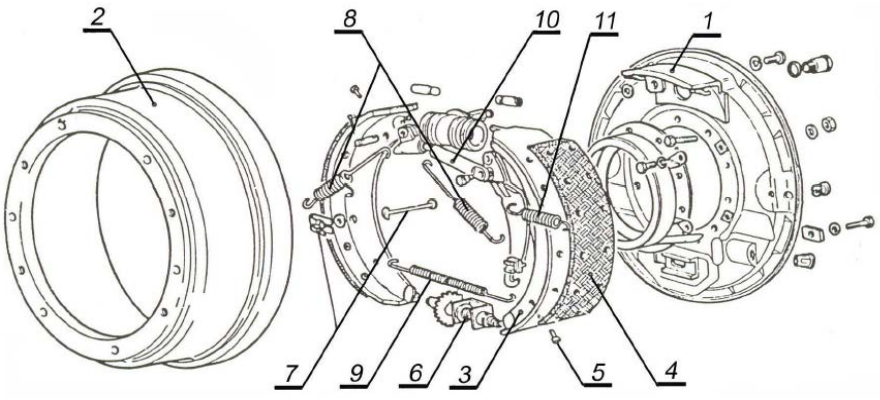

Figure 1 Main parts of rear drum brakes

1 – Baking plate, 2 - Drum, 3 – Brake shoe, 4 – Shoe lining, 5 - Rivet, 6 – Brake adjuster, 7 - Elements for holding the shoes, 8 - Shorter return spring, 9 - Longer return spring, 10 – Lever mechanism of the parking brake 11 - The return spring

Main task of elements for holding shoes (7) is to ensure the specific position of shoes, so during brakes activating, the brake is as quickly and better brought into contact with the drum. Return springs (8) and (9) hold the shoes attached to the supports and during releasing they return shoes to the starting position Rear brakes of the vehicles represent the executive mechanisms of the service and parking brake of the vehicle. Activation of shoes for the parking brake is done via the lever mechanism (10). After termination of the parking braking, spring (11) returns a lever mechanism for activation of the drum brake in the position prior to activation [1]. Brake pads are important part of braking systems for all types of vehicles that are equipped with disc brakes. They are considered as one of the key components for the overall performance of a vehicle and as heterogeneous materials, they are usually made from more than 10 ingredients. An ideal brake friction material should have constant coefficient of friction under various operating conditions such as applied loads, temperature, speeds, mode of braking and in dry or wet conditions so as to maintain the braking characteristics of a vehicle

1.1 Statement of the Problem

The study for wear, hardness and thermal analysis drum brake and liner has become a strong need for this work. In this paper using software such as (ANSYS Workbench, and SOLID WORK) study mechanical and thermal property for two different drum brake numerically and finally comparing the results. Also investigate the performance and wear properties of commercial brake liner and local brake liners by goings on AWASH ARABA BRAKE PAD AND LINING FACTORY (AABPALF) using by Jf 150 friction material waer test machine,rock well hardness and chase test machines. From my surveying of the passenger cars are mainly used drum brakes at the rear wheels of the vehicles. Most of the small vehicles like Toyota hiaces are widely used in our country the rear wheel of the outer surface of brake drums product are flat. Due to emergency braking the temperature is become maximum and the deformation is it may happen. From this problem I have to focus and investigate on this area especially in Ethiopia to much passenger car (Toyota hiace) are available. Most of the time the applied brake is in small distance the range between 50-100 meters. By the consideration of this applied brake it may happen some problems due to temperature and other mechanical systems.

2 Literature Review

Table 1 relevant papers

Publishing Year and Authors	Titles of the Project	Discussion
Dvsrbm Subramanyam.Sravani (2017)	DESIGN AND ANALYSIS OF DRUM BRAKES	study the thermal analysis of drum brake with three different materials aluminum alloy, Carbon Steel, aluminum Metal matrix at 90^0c temperature and 22^0c ambient temperature of convection is applied conclude that beside general material, aluminum metal matrix (ks1275) which is economically less cost and less weight ratio [2].
Anup Kumar and R. Sabarish 2004	Structural and Thermal Analysis of Brake Drum	Study on the thermal stresses and mechanical stresses together And conclude that from the transient temperature it is observed that the temperature is increasing with each cycle.it shows that the cooling time provided is not sufficient to cool the drum. The design check has been done by comparing the maximum obtained stress, It was found that the design is safe and the brake drum functions properly under the given load conditions [3].
Silveira Z.C et al.(2014)	Thermal Analysis of a Rear Drum Brake for Lightweight Passenger Vehicles	**S**tudied the thermal analysis of a sub-set drum/shoe brake lining of a braking system in a rear drum brake for a lightweight passenger vehicle with engines of up to 1,000 cc. Numerical results show the transient temperature filed in the lining during different types of braking processes, such as once emergency braking, continuous downhill braking and repetitive braking. The maximum temperature reached on the lining surface was 375.64 ˚C for the continuous downhill braking case after 200 s of braking at 60 km/h, considering a 10% slope [4].
Ehtisham Shahid1, Xiaoying Wang1, Zijie Fan1, Liangjin Gui1(2018)	Numerical Simulation of the Stress, Temperature & Wear Behaviors of the Drum Brake	Study the Archard abrasive wear model and Finite Element Method (FEM) are combined to simulate the normal braking condition of drum brake by means of the stress and wear coupled analysis method And his concludes that contact pressure of leading shoe is larger than the trailing shoe. The contact pressure at the both ends of the both shoes are higher than the middle area [5].

3 Material and Methods

In this section the specification is taken from online Toyota hiace I Wagon Company. The materials used in this analysis direct imported and selected on Solid works, the mechanical models such as normal and a finned brake drum model developed using this software. The properties of the brake drum material (gray cast iron) are shown in table 3 below. In the analysis, SOLIDWORKS modelling and simulation methodology has been employed to develop and study the impact of forces and thermal stress acting on the normal and finned brake drum model and some properties are analysis by ANSYS Workbench.

Properties of the Brake Drum

1. Must have a hard wear-resistant rubbing surface and surface finish must not damage the lining.
2. Must be strong enough to withstand the hardest braking while at high temperature.
3. Must be stiff and resistant to distortion and warping

4. Must dissipate heat rapidly and withstand excessive temperature. The detail of Toyota hiace specification in the appendix G below.

3.1 Static and Dynamic Analysis

A. Assumptions

In developing the equations, the following assumptions have been made;

- The pressure at any point on the shoe is proportional to the moment arm of this point from the pivot.
- The effect of centrifugal force may be neglected.
- The shoe is assumed to be rigid.
- The friction coefficient is a linear function of temperature and it does not vary with pressure, wear and environment.

B. Brake force distribution

Braking-force proportioning device is used to adjust the apportionment of the braking force between front and rear axles as determined by the brakes' particular dimensions in order to achieve a closer approximation to the ideal distribution.

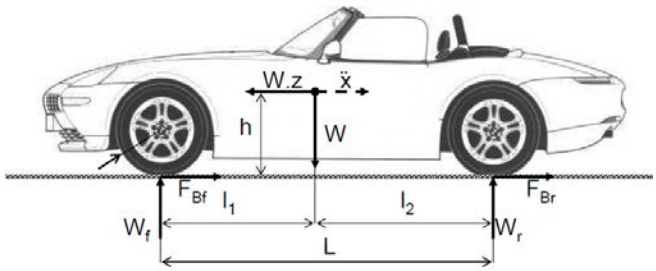

Figure 2 force acting on the vehicle during braking *[6]*

For a conventional brake system, the distribution of the braking forces is primarily dependent on the hydraulic or pneumatic pressures, brake geometry and brake cylinder areas in the front and rear brakes.
During braking, a dynamic load transfer from the rear axle to the front axle occurs such that the load on an axle is the static plus the dynamic load transfer. Neglecting, the road resistances, from Figure 3, front and rear axle loads can be calculated as [6].

$$Wf=\frac{W}{L}(l2 + z.h) \text{ and } Wr=\frac{W}{L}(l2 - z.h) \quad (1)$$

Where z is non-dimensional deceleration

$$Z = \frac{-\ddot{x}}{g} \quad (2)$$

From the force balance in longitudinal axis is $F\,bf + F\,br = W.z$
Thus

$$\frac{FBf}{W}+\frac{FBr}{W} = z \quad (3)$$

According to EC regulations, for passenger cars, rear tires should not lock up between decelerations of 0.15 g and 0.8 g and 5 % tolerance is allowed between 0.3 g and 0.45 g. Also, in order to satisfy the stopping distance requirements, installed braking force distribution should be above the curve determined by:

$$\frac{F_{Bf}}{W}=\frac{Z+0.07}{0.85}\left(\frac{l_2}{L} - z\frac{h}{L}\right) \text{ where; } (z = 0.15 \ldots. z = 0.61) \quad (4)$$

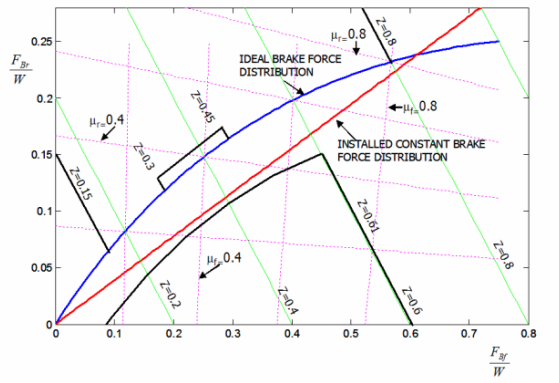

Figure 3 Brake force distribution diagram and EC regulations [7]

C. Pressure Concept

To analyze an internal-shoe device, refer to Fig.5, which shows a shoe pivoted at point *A*, with the actuating force acting at the other end of the shoe. Since the shoe is long, we cannot make the assumption that the distribution of normal forces is uniform. The mechanical arrangement permits no pressure to be applied at the heel, and we will therefore assume the pressure at this point to be zero. It is the usual practice to omit the friction material for a short distance away from the heel (point *A*). This eliminates interference, and the material would contribute little to the performance anyway, as will be shown. In some designs the hinge pin is made movable to provide additional heel pressure. This gives the effect of a floating shoe [8].

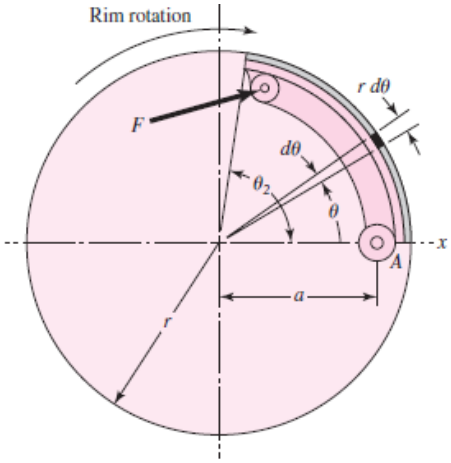

Figure 4 Internal friction shoe geometry.

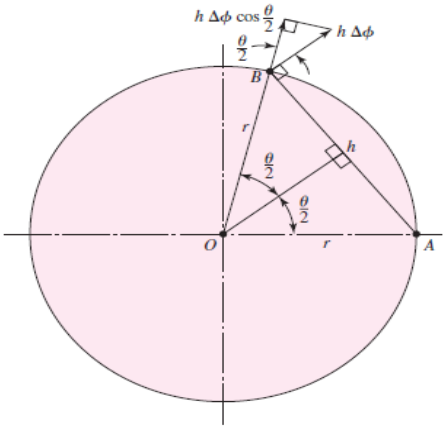

Figure 5 the geometry associated with an arbitrary point on the shoe

Let us consider the pressure *p* acting upon an element of area of the frictional material located at an angle θ from the hinge pin (Fig.5). We designate the maximum pressure P_a located at an angle θ*a* from the hinge pin. To find the pressure distribution on the periphery of the internal shoe, consider point *B* on the shoe (Fig.6). If the shoe deforms by an infinitesimal rotation Δφ about the pivot point *A*, deformation perpendicular t to *AB* is *h* Δφ. From the isosceles triangle AOB, h = 2 r sin (θ/2), so

$$h\,\Delta\varphi = 2\,r\,\Delta\varphi \sin(\theta/2) \quad (2)$$

The deformation perpendicular to the rim is *h* Δφ cos (θ/2), which is

$$h\,\Delta\varphi \cos(\theta/2) = 2\,r\,\Delta\varphi \sin(\theta/2)\cos(\theta/2) = r\,\Delta\varphi \sin\theta \quad (3)$$

Thus, the deformation, and consequently the pressure, is proportional to sin θ. In terms of the pressure at *B* and where the pressure is a maximum, this means

$$\frac{P}{sin\theta} = \frac{Pa}{sin\theta a}$$

Rearranging gives

$$p = \frac{Pa}{sin\theta a}\sin\theta \quad (7)$$

From this formula it can be seen that the frictional material at the heel, contributes very little to the braking action, therefore it is better to begin the friction material at an angle Θ_1 greater than, say 0.15 rad. It can be seen also that the pressure will be maximum when Θ =90° or if the toe angle Θ_2 is less than 90°, then the pressure will be maximum at the toe. For good performance it is recommended to concentrate as much frictional material as possible in the neighborhood of the point of maximum Pressure

D. Actuating Force and Torque Calculation

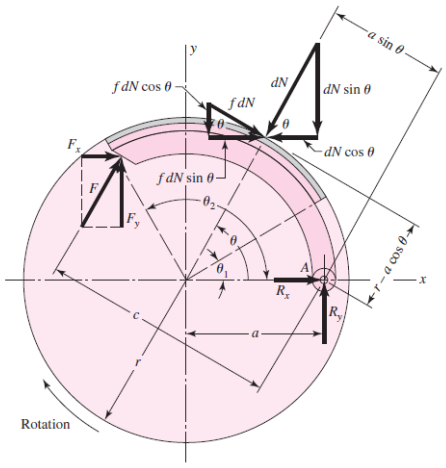

Figure 6 force on shoe

Proceeding now (Fig.6), the hinge-pin reactions are *Rx* and *Ry*. The actuating force *F* has components *Fx* and *Fy* and operates at distance *c* from the hinge pin. At any angle θ from the hinge pin there acts a differential normal force *dN* whose magnitude is *dN* = *pbr dθ* where *b* is the face width (perpendicular to the paper) of the friction material. Substituting the value of the pressure from Eq. (3.7), the normal force is

$$dN = \frac{P_a br \sin\theta\, d\theta}{siin\theta_a} \quad (8)$$

The frictional forces have a moment arm about the pin of $r - a\cos\theta$. So, the moment *Mf* of these frictional forces is

$$Mf = \int f\, dN(r - a\cos\theta) = \frac{f\, P_a br}{siin\theta_a}\int_{\theta 1}^{\theta 2} \sin\theta(r - a\cos\theta)\, d\theta \quad (9)$$

The moment of the normal forces by (*Mn) is calculated by*

$$Mn = \int dN(a\sin\theta) = \frac{P_a bra}{siin\theta_a}\int_{\theta 1}^{\theta 2} sin^2\theta d\theta \quad (10)$$

The actuating force *F* must balance these moments. Thus

$$F = \frac{M_N - M_f}{c} \quad (11)$$

The torque T applied to the drum by the brake shoe is the sum of the frictional forces $f\,dN$ times the radius of the drum:

$$T = \int frdN = \frac{f\,P_a br^2}{sin\theta_a}\int_{\theta 1}^{\theta 2} sin\,\theta d\theta = \frac{f\,P_a br^2(cos\,\theta 1 - cos\,\theta 2)}{sin\theta_a} \quad (12)$$

3.2 Wear

An interaction between a drum brake and pads of automotive brake is characterized by a number of dry contact phenomena. These phenomena are influenced by brake operation conditions (applied pressure, speed, and brake interface temperature) and material characteristics of a friction couple. The coefficient of friction should be relatively high and keep a stable level irrespective of temperature change, humidity, age, degree of wear and corrosion, presence of dirt and water spraying from the road. During braking surface temperature generated in contact areas has a major influence on wear, scuffing, material properties and material degradation. Due to these reasons, this thesis focuses on surface wear analysis of drum brake. Wear, according to Bayer, is defined as "damage to a surface as a result of relative motion with respect to another substance". For the purposes of this work, wear shall be defined as the loss of material from a surface due to sliding along another surface. Two methods of classifying wear are: (1) the conditions in which the wear occurs; and (2) the mechanism by which the wear occurs. Conditions used to classify wear include whether or not there is a lubricant present, and whether or not there are hard, abrasive particles present. If there is a lubricant present, it is referred to as lubricated wear, otherwise it is dry wear. If there are abrasive particles causing wear, then it is referred to as abrasive wear, otherwise it is called sliding wear. The numerical integration of wear is based on the Euler method. The incremental form of generalized Archard wear model is.

$$\Delta h = kp\Delta s \quad (13)$$

In the above formation Δh is the increment for wear thickness, k is the coefficient for wear factor,
Δs is the increment for relative displacement. By assuming the contact nodes of the brake drum and the friction plates in finite element mesh is i and the integration step is j then the wear increment is as followed. *[5]*

$$\Delta h(I,j) = k(I,j)p(i,j)\Delta s(I,j) \quad (14)$$

Then the cumulative wear is appeared as,

$$h(I, j) = \sum_{i=1}^{j} h(i,j) \sum_{i=1}^{j} k(i,j)p(i,j)\Delta s(i,j) \quad (15)$$

3.3 Stress distribution of drum brake

To calculate the stress in the Brake Drum by the application of pressure. Stress is resistance offered by the body to deformation. Generally, maximum pressure acts on trailing side of Brake Drum. We know that, if the thickness to diameter ratio (t/D ratio) is 1/10 to 1/20 then the cylinder can be considered as thin cylinder. [9]

Hoop Stress (σ_h) is

$$\sigma_h = (PD/2t) \quad (16)$$

Longitudinal Stress (σ_L)

$$\sigma_L = (PD/4t) \quad (17)$$

Von Miss Stress

$$\sigma = (\sigma_h^{\,2} + \sigma_L^{\,2} - 2(\sigma_h \times \sigma_L))\ \text{^}1/2 \quad (18)$$

In thin cylinders, the stresses in radial direction are zero, i.e. σr = 0
And the total deformation is calculated as;

$$\Delta D = [D \times (\sigma h - \boldsymbol{\mu}\sigma_L)]\ /E \quad (19)$$

3.4 Rate of Heat Generated and Deceleration Calculation

The differential rate of heat generated by an element area of the lining is equal to the velocity of the inside surface of the drum relative to the lining, times the differential frictional force acting on the element area;

$$dQ = V_r\,df \quad (20)$$

Assuming the brake is on a vehicle wheel with a radius of R, the inside surface velocity is equal to;

$$V_r = \frac{r}{R}v \tag{21}$$

Where V is the velocity of the vehicle and is a function of time. If v = v (t) then $v_r = v_r$ (t) and the heat generated will be also a function of time. Substituting the values of v_r and df and integrating from Θ1 to Θ 2 we get the following formula for the heat generated at any time t.

$$Q(t) = \frac{P_a bu}{siin\theta_a}\left(\frac{r}{R}\right)^2 (\cos\Theta_1 - \cos\Theta_{2)\,V}\ (t) \tag{22}$$

The kinetic energy of a vehicle of weight W is given by;

$$E = \frac{1}{2}\left(\frac{w}{g}\right)v^2 \tag{23}$$

Mote that if the brake is on a four wheel vehicle, there will be eight shoes. Assuming all are leading shoes, each will stop one-eighth of the vehicle weight, so W/8 must be used. The rate of change in the kinetic energy is;

$$\frac{dE}{dt} = \left(\frac{w}{g}\right)v\frac{dv}{dt} \tag{24}$$

From the energy conservation law the rate of change in the kinetic energy is equal to the heat generated;

$$Q(t) = \frac{dE}{dt} \tag{25}$$

Substituting the value of Q (t) and dE/dt, it is seen that the velocity v (t) cancels and so the deceleration is not a function of time. Therefore the deceleration, dc, is;

$$dc = \frac{dv}{dt} = \left(\frac{g}{w}\right)\frac{P_a bu}{siin\theta_a}\left(\frac{r}{R}\right)^2 (\cos\Theta_1 - \cos\Theta_{2)} \tag{26}$$

The velocity at any time is;

$$V = V_i - dct \tag{27}$$

Where v_i. Is the initial velocity. Substituting the velocity in Equation (a), yields the rate of heat generated as a function of time,

$$Qt = \frac{P_a bu}{siin\theta_a}\left(\frac{r}{R}\right)^2 (\cos\Theta_1 - \cos\Theta_{2)\,(}Vi - dct) \tag{28}$$

In this study the friction coefficient was taken as constant up to a temperature of 90°C and after 90°C, decreases linearly to zero at a specified temperature, T_{max}.

$$\mu = \begin{cases} \mu_c & T \le 90^0 c \\ \mu_{c-}\frac{\mu c - \mu h}{\Delta h}(T - 90) & 90^0 c < T \le T_{max} \\ 0 & T \ge T_{max} \end{cases}$$

Where μc is the cold coefficient of friction and μh is the hot coefficient of friction.

3.5 Surface Temperature Calculation

Since the function of a brake is to convert kinetic energy into heat, surface temperatures of brake linings and drums are most important. Therefore it is necessary to know the temperature of the mechanism during and after any stop. The temperatures were calculated by the finite difference method.

1. Assumptions

a. One dimensional heat flow-the heat flow is from the inner surface to the outer surface of the drum.
b. Constant heat transfer coefficient.
c. No heat dissipated by radiation.

d. The heat is generated on the inner surface.

2. Temperature Analysis

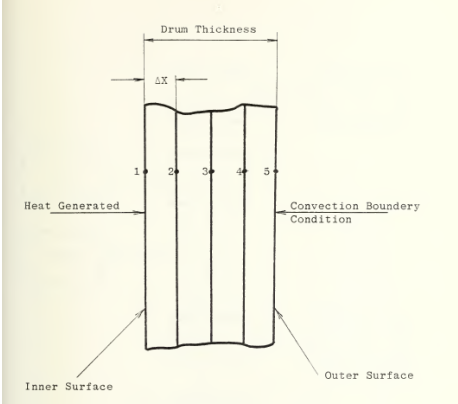

Figure 7 Finite Difference Model

The differential equation to be solved in order to find the temperature in the drum, based on the

Assumptions, is;

$$\frac{\partial^2 T}{\partial x^2}+\frac{Q}{K}=\left(\frac{1}{a}\right)\frac{\partial T}{\partial t} \tag{29}$$

With the following boundary conditions:

- ✓ At x=0 heat is generated,
- ✓ At x=tk heat is transferred to the atmosphere by convection.

In the equation above k is the thermal conductivity, a is the thermal diffusivity, t is time and tk is the drum thickness. This equation can be solved by the finite difference method [10].The finite difference model used here is shown in Fig.7. The rate of change with time of the internal energy of a node i is approximated by;

$$\frac{\Delta E}{\Delta t}\geq \rho c \Delta V_0 \frac{T_i^{P+1}-T_i^P}{\Delta t} \tag{30}$$

Where ρ the density, c is is the specific heat and V_0 is the drum volume. Now define the thermal capacity as

$$C_i=\rho_i c_i \Delta V_{0_i} \tag{31}$$

3.6 Transient Thermal Analysis

This model is run as a transient analysis because I want to study the heat distribution during braking from a selected speed of 14m/s, 17 m/s and 25 m/s to a complete stop. It can easily calculate the time it takes to stop by first calculating the force it takes to stop the vehicle. From the vehicle specification (detailed in Appendix I B) that the Gross car weight is 1800 kg and assume the coefficient of friction between asphalt and rubber is 0.72. To stop the vehicle in the shortest time, the maximum breaking force cannot be larger than the maximum friction force between the tires and the ground, which can be transmitted to the ground. This maximum friction force is calculated as follows.

$$F_f = \mu \times m \times g \tag{32}$$

$$(0.72)(1800kg)\ (9.81m/s^2) = 12713.76\text{N}$$

The average acceleration of the car during braking is calculated as follows.

$$\alpha_x = F_f/m \tag{33}$$

$$\alpha_x = 12713.76\text{N}/1800\text{kg} = 7.06 m/s^2$$

Finally, we can calculate the time it takes to stop.

$$t=\frac{v_x}{a_x} \quad (34)$$

For the speed of 50km/hr the time is

$$t=\frac{13.88m/s}{7.06m/s2}=1.966\text{sec}\approx 2\text{sec}$$

For the speed of 60km/hr and 90km/hr the time is t=2.36sec and 3.54sec respectively.

Note: - this time is used to input time curve on transient analysis

3.6.1 Thermal Boundary Conditions

SolidWorks Simulation solves for the temperature distribution in the solid using the conduction equations and boundary conditions applied to the boundaries of the model. SolidWorks Simulation has several thermal boundary conditions that can be applied to thermal studies.

- **Temperature**

Allows for the definition of a temperature on a certain entity or body.

- **Convection**

Applies a convection boundary condition to the selected faces. The convection coefficient and ambient temperature are specified and the heat lost due to convection is calculated automatically.

- **Heat Flux**

Applies some amount of heat into a face per unit area.

- **Heat Power**

Applies some amount of heat to a vertex, edge, face or component.

- **Radiation**

Allows surface-to-surface or surface-to-ambient radiation. In this model, apply convection to all faces because all of the faces will be exposed to the air. In addition, we will apply a heat power to the faces that the brake line and drum touch.

3.6.2 Convection Boundary Conditions

Amount of heat transferred through conduction is proportional to the convection coefficient, *h*, the surface area, *A*, and the temperature difference between the surface and the surrounding fluid.

$$Q_{convection}\ (q''conv) = h\ A\ (Ts - T\infty) \quad (35)$$

Where *Ts* and *T*∞ are the temperatures of the bounding surface and fluid, respectively. This expression is known as Newton's law of cooling, in this lesson, we will assume a convection coefficient of 230W/m^2 ^{0}C and an ambient temperature of 22°C, which are approximations. Actual convection coefficients and ambient temperature could be computed by running a CFD analysis in SolidWorks Flow Simulation or from experiments.

3.6.3 Radiation Boundary Conditions

Thermal radiation is the energy transported by electromagnetic waves emitted by matter at a nonzero temperature. The rate per unit area at which the energy is emitted by a surface is known as emissive power *E*, given by equation

$$E = \varepsilon\sigma T_S \quad (36)$$

where *Ts* is the absolute temperature of the surface, ε is a radiation property of the surface, called emissivity ($0 \le \varepsilon \le 1$) and σ is the Stefan-Boltzmann constant (σ = 5.67x10-8 *W/(m²K4.)*).However, a surface does not only emit radiation; it may also be incident to the surface from the surroundings and a portion or all incident irradiation may be absorbed by the surface.

$$G\ abs = \alpha G \quad (37)$$

Where α is a irradiative property of the surface termed absorptive and *G* is the total radiation incident to the surface. In other words, α is the portion of the irradiation that is absorbed by the surface, thus $0 \le \alpha \le 1$.

The net rate of the heat transfer by radiation that leaves the surface is expressed by equation

$$q"rad = \varepsilon E - \alpha G \quad (38)$$

Considering a specific case in which $\alpha = \varepsilon$ (a gray surface) and replacing equations (36) and (37), equation (38) becomes:

$$q"rad = \varepsilon\sigma (T_S^4 - T_{sur}^4) \quad (39)$$

3.7 Heat Power

As the vehicle is braked creating friction and heat energy. Much of the kinetic energy of the car is being transferred to thermal energy through the brake lines. The heat power will be applied to the brake drums in the area that the liners touch. The amount of heat power can be calculated from the amount of kinetic energy carried by the car. The mass of the car is 1800 kg and the car is travelling at different speed such as (50, 60 and 90) km/hr, the kinetic energy of the car is as follows:

$$KE=\frac{1}{2}mv^2 = \frac{1}{2}1800\times(13.88)^2 = 1.733\times10^5 \text{ J (for 50 km/hr)},$$
$$2.498\times10^5 \text{ J (for 60 km/hr)}$$
$$\text{And } 5.625\times10^5 \text{ J (for 90 km/hr)}$$

If we assume all of that kinetic energy is transferred to thermal energy during braking that lasts 3seconds, we can calculate the heat power.

$$\text{Heat power} = \frac{KE}{\Delta t} = \frac{173.3kJ}{3s} = 57.76\text{kW}$$

For 60 and 90km/hr the heat power is 83.266kWand 187.5kW respectively.

Since we will analyze only one liner, and about 40% of the mass of the vehicle will be on the rear, the heat power is reduced.

$$\text{Heat power} = \frac{KE}{\Delta t} = \frac{57.76\ kW\times0.4}{2} = 11.552\text{kW (for 50km/hr)}$$

$$\frac{83.266kW\times0.4}{2} = 16.65\text{kW (for 60km/hr)}$$

$$\frac{187.5\ kW\times0.4}{2} = 37.5\text{kW (for 90km/hr)}$$

Note:-This analytical result is used to as input for applied thermal load on the drum and friction plate.

3.8 2D model representation of friction plate, finned &normal drum brake

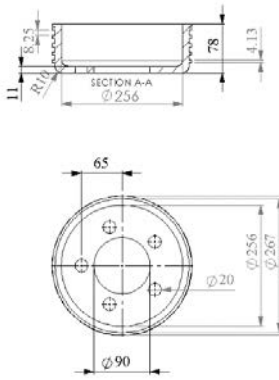

Figure 8 2D model of finned drum

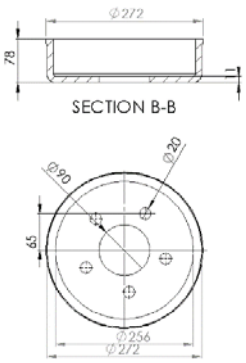

Figure 9 2D model of normal drum

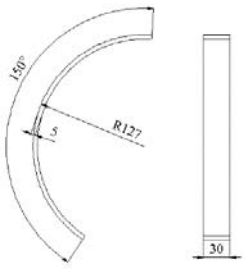

Figure 10 2Dmodel of friction plate

3.8.1 Gray Cast Iron Material Composition and Thermo-Elastic Properties

A drum brake is generally made from gray cast iron due to cast iron provides good wear resistance with high thermal conductivity, high thermal diffusivity, and low production cost compared to other drum and disc brake rotor materials such as AL-MMC, carbon composites and ceramic based composites . Due to this reason it is a material that has been commonly used to create components of varying complexity for a long time. Gray cast iron's high damping capacity, combined with its excellent machinability and high hardness, is unique to this material and makes it ideally suited for machine bases and supports, engine cylinder blocks and brake components.

Table 2 Gray Cast Iron properties

property	value	Units
Elastic modulus	66178.1	M/mm^2
Poisson's ratio	0.27	N/A
Shear modulus	50000	N/mm^2
Mass density	7200	Kg/m^3
Tensile strength	151.658	N/mm^2
Compressive strength	572.165	N/mm^2
Yield strength		N/mm^2
Thermal expansion coefficient	1.2e-005	/k
Thermal conductivity	45	W/(m.k)
Specific heat	510	J/(kg.k)
Material damping		N/A

Note:-the above material properties are direct input from SOLIDWORK

4 Result and Desiccation

4.1 Numerical Analysis

Figure 11 3D model of normal and finned drums

A. Meshing

Three dimensional model (3D) of drum brake is performed in Solid work and the profile is subdivided into nodes and elements. Collection of elements is called mesh and it is necessary to make mesh optimization to get more accuracy results. Mesh optimization is carried out until the *FEA* results and analytical solutions are close to each other. Meshing of Model: We discretized the solid model into small elements. Depending upon the requirement of the accuracy of results the fineness of meshing varies. This meshing varies used is 8mm, 6mm, 4mm, 3mm, 2mm, 2.5mm and 1.5mm,. Finer is the meshing more we are closer to the actual results and when mesh size increases maximum stress on the component become decreased

Table 3 meshing information for finned drums

	Mesh with Element size 3	Mesh with Element size 2.5	Mesh with Element size 2	Mesh with Element size 1.5
Meshing with different element size	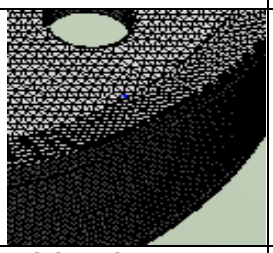	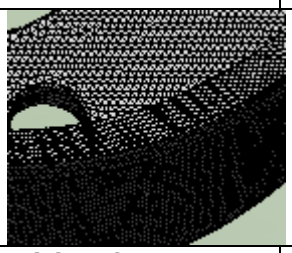	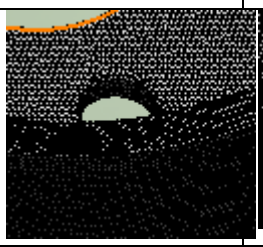	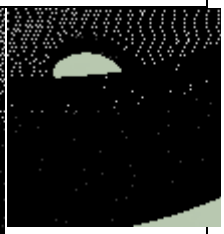
Mesh type	Solid Mesh	Solid Mesh	Solid Mesh	Solid Mesh
Mesher Used:	Standard mesh	Standard mesh	Standard mesh	Standard mesh
Total nodes	452969	727857	1334685	3162201
Total elements	298284	487437	911564	2213431
Element Size	3mm	2.5mm	2mm	1.5 mm
Tolerance	0.15mm	0.125mm	0.1mm	0.075mm
Mesh Quality	High	High	High	High
Maximum aspect ration	12.963	11.206	10.988	9.2486
% of elements with Aspect Ratio < 3	98.9	99.3	99.3	99.6
Time to complete mesh (hh; mm; ss):	00:00:32	00:01:34	00:03:45	0:12:12
Computer name and specifications	Hp, core i5-4200Mcpu@2.50Hz , installed RAM:4.00GB			

Table 4 meshing information for finned drums

	Mesh with Element size 3	Mesh with Element size 2.5	Mesh with Element size 2	Mesh with Element size 1.5
Meshing with different element size	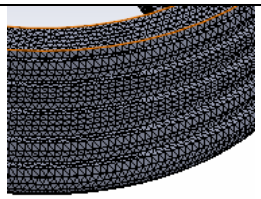	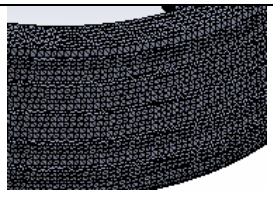	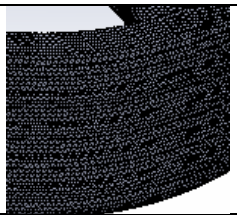	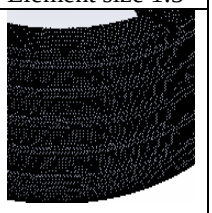
Mesh type	Solid Mesh	Solid Mesh	Solid Mesh	Solid Mesh
Mesher Used:	Standard mesh	Standard mesh	Standard mesh	Standard mesh
Total nodes	331780	496575	958099	2089844
Total elements	215502	327036	648267	1448982

Element Size	3mm	2.5mm	2mm	1.5 mm
Tolerance	0.15mm	0.125mm	0.1mm	0.075mm
Mesh Quality	High	High	High	High
Maximum aspect ration	9.1867	7.5007	6.7929	8.257
% of elements with Aspect Ratio < 3	99.4	99.5	99.6	99.7
Time to complete mesh (hh; mm; ss):	00:00:24	00:0:45	00:02:00	00:06:13
Computer name and specifications	Hp, core i5-4200Mcpu@2.50Hz , installed RAM:4.00GB			

Note: in this table to take four finer meshing size

4.1.1 Simulation and Analysis

The amount of friction developed between the two surfaces in contact is independent of the area of the surface in contact. However the magnitude of the force of friction or retarding force created between the brake lining and the brake drum depends upon the pressure or force exerted on the shoes by the retarding mechanism and the coefficient for the two materials. For this paper, a retarding force of 4996N is considered to be acting between the brake lining and the brake drum. The comparison between the normal and the finned model is due to considering the mechanical properties and thermal properties of both model surface with the same boundary conditions.

- Static Analysis of the normal drum brake

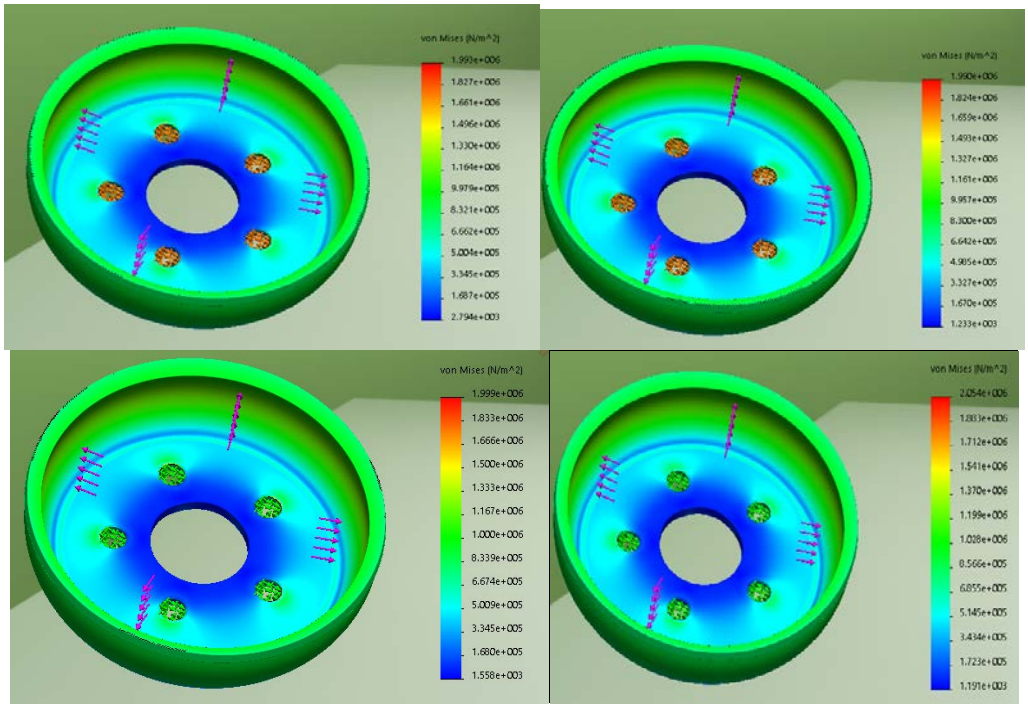

Figure 12 von-mises stress comparison results of normal drum brake

Note:-This analysis study seven statics analysis starting from the element size (8,6,4,3,2.5,2 and 1.5) this comparetion pick only more fine mesh size. i.e elemnt size 3 to 1.5.

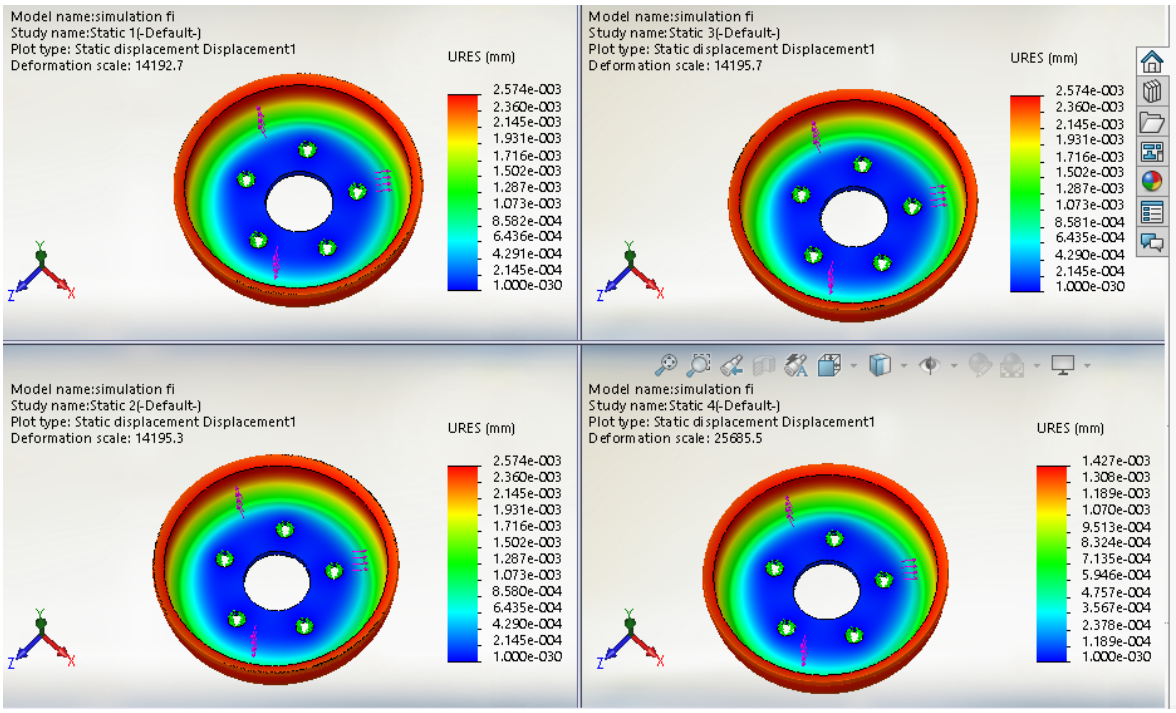

Figure 13 comparison of total deformation

✓ The mesh independence for normal drum brake is discribed below the graph :

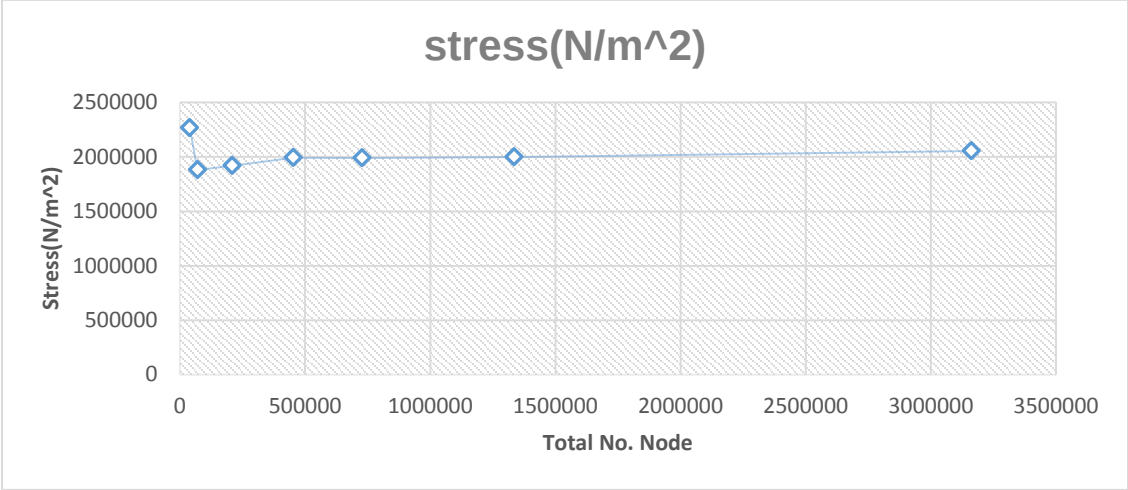

Figure 14 mesh independence of normal drum

This mesh independence graph shows when the element size is more decrease the line is almost it become linear and the value is accurate.

➢ Static Analysis of the finned drum brake

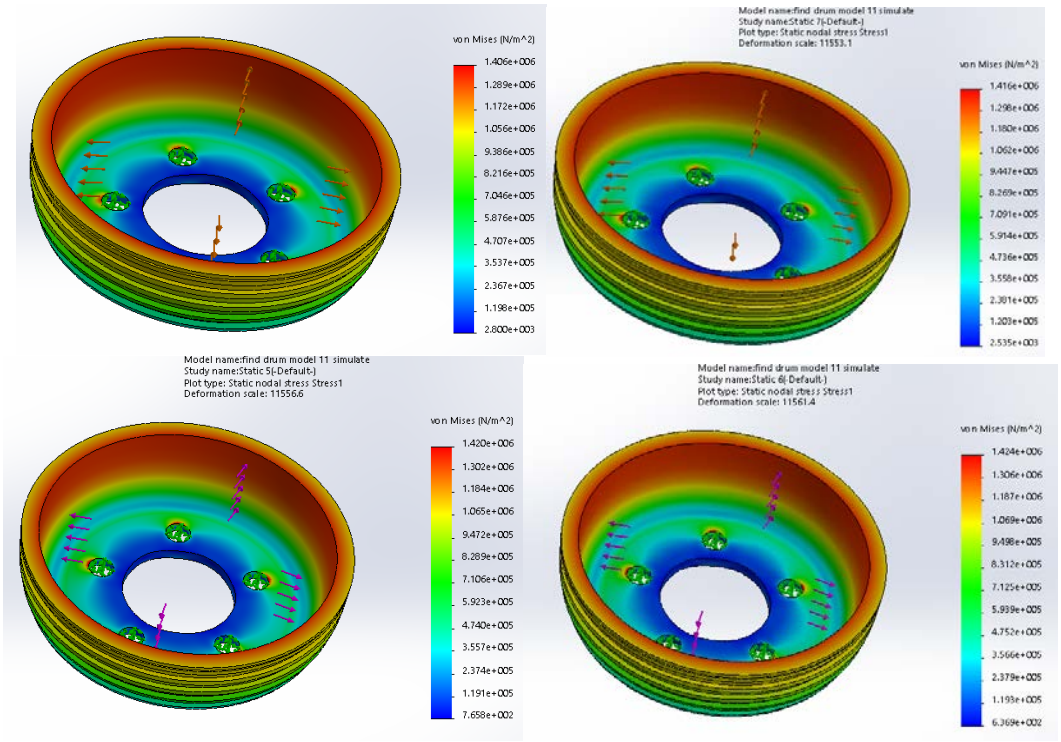

Figure 15 von-mises stress comparisons result of finned drum brakes

Note:-This analysis study seven statics analysis starting from the element size (8,6,4,3,2.5,2 and 1.5) this comparetion pick only more fine mesh size. i.e elemnt size 3 to 1.5.

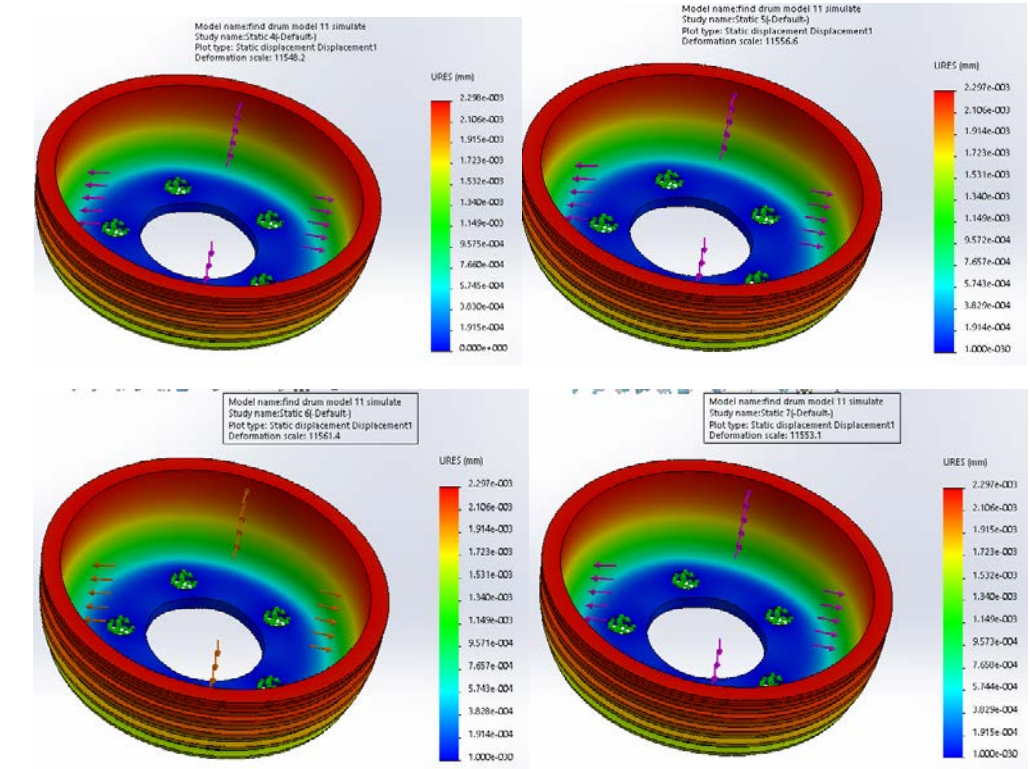

Figure 16 Total deformation of finned drum brake

✓ The convergence criteria for finned drum brake is discribed below the graph :

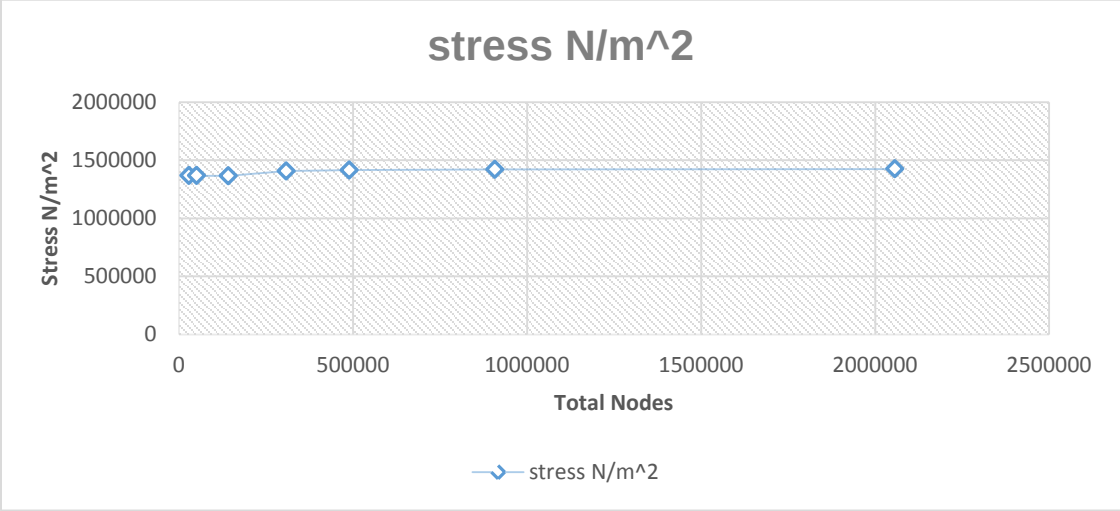

Figure 17 Mesh independence of finned drum

This mesh independence graph shows when the element size is more decrease the line is almost it become linear and the value is accurate.

The results of this normal and finned type drum brake is shows the normal drum brake of von-misses and displacement is greater than the finned drum brake this indicate that the finned drum brake is high strength and less deformation as compare to the normal one.

4.1.2 Steady -state thermal analysis of both normal and finned drum brake

In this analysis I have to take the same common initial input data for using analysis of total heat flux and temperature distribution used to comparison between those two different drum brake models

Heat flux	23000 w/m^2
Convection	230 w/m^{2o}c
Radiation to atmosphere	22^{o}c

➢ Analysis of thermal on Drum Brakes by using ANSYS 18.1 WORK BENCH software

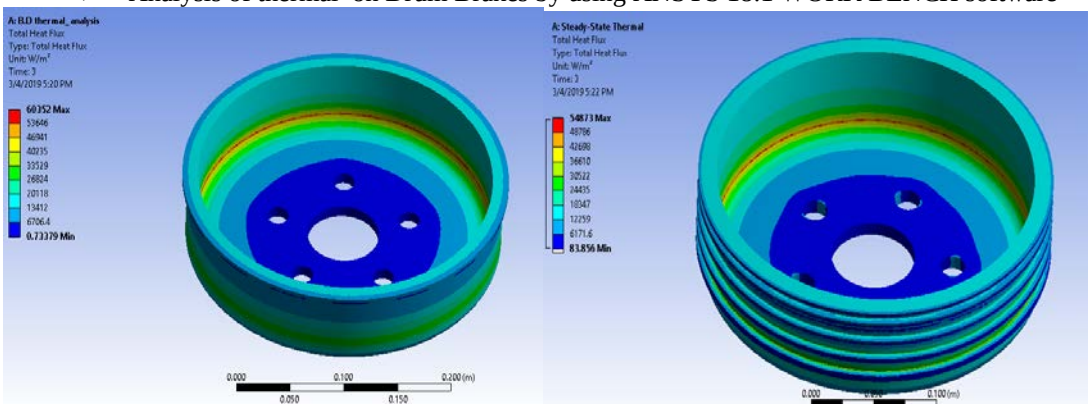

Figure 18 heat flux Analysis

Normal drum brake	**Min**	**Max**
Total heat flux	0.7337 w/m^2	60352 w/m^2
Finned drum brake	Min	Max

Total heat flux	83.856 w/m^2	54873 w/m^2

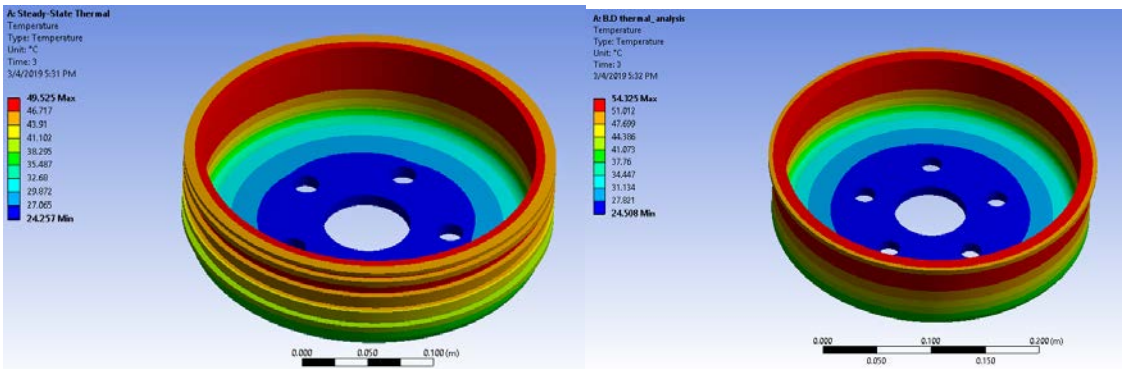

Figure 19 temperature results of drum brakes

Normal drum brake	**Min**	**Max**
Temperature	24.508^{o}c	54.325^{o}c
Finned drum brake	Min	Max
Temperature	24.257^{o}c	49.525^{o}c

- Thermal analysis on Friction plate

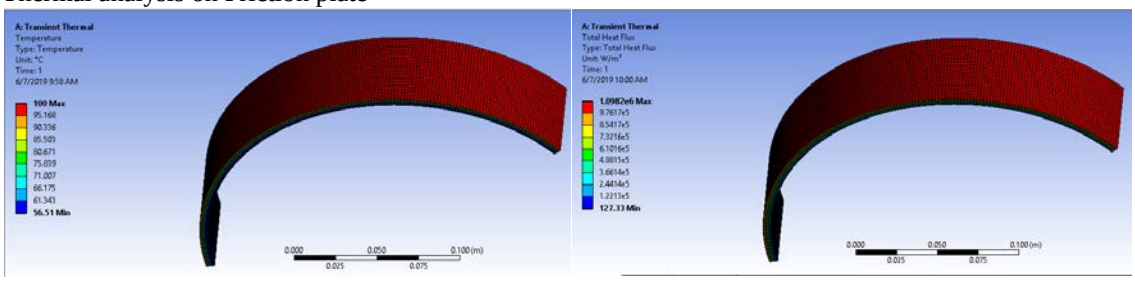

Figure 20 temperature results of friction plate

drum brake friction material	**Min**	**Max**
Total heat flux	127.33W/m^2	1.0982e+006W/m^2
Temperature	56.51^{o}c	100^{o}c

Fatigue Life

This result contour plot shows the available life for the given fatigue analysis. If loading is of constant amplitude, this represents the number of cycles until the part will fail due to fatigue. If loading is non-constant, this represents the number of loading blocks until failure.

Table 5 fatigue life of drum brake and lining

Fatigue Life Of Drum Brake And Liner		
Models	**Minimum Life**	**Max Life**
Normal Drum Brake	4.072e+005	1.e+006
Finned Drum Brake	5.4035e+005	1.e+006
Friction Plate	1178	1.e+006

4.2 Experimental results and desiccation

4.2.1 Sample Preparation

The sample Brake friction plate get from Ethiopian auto spare part llc of three different brake liner such as Brazil, china's and Mintex brake liner with comparison of local products. The sample is prepared depend on the available test machine such as rock well hardness test machine, friction and wear rate test machine and chases test machine with the same standard of sample. The sample size is cut on grinding machine in the square form of dimension 25*25mm and thickness size approximate to 6mm. The end surfaces of pin finished on sand paper or the sample thickness is large smoothing by grinding wheel to ensure the size of sample is aligned with square box during rotating motion. The finished brake pad material as shown in following figure prepared as.

Figure 21 sample friction plate

4.2.2 Hardness Lab Testing

After the brake pads were constructed a hardness test was to be conducted. The hardness test used was Rockwell hardness test. This was preferred because; it can be used for non-metals, indenters are small hence it could not destroy the specimen, it is a high speed test and the surface does not have to be reflective This test consists of an indenter which is a diamond cone with an angle of 120^0 and a tip radius of 0.2mm or steel balls of various diameters. The Ethiopia Metals and Engineering Corporation (METEC) standard for this test is XHR-150 Rockwell hardness tester. The overall specification is put on the Appendix IG. The test was done on different five positions of the sample for all commercial (Brazil, Mintex and china's brake liner) and local METEC brake liner specimen and an average reading recorded.

Figure 22 Rock well hardness test machine

The Rock well hardness test of different commercial products including local products the test was done on different five positions the results as follows.

Table 6 Rock well hardness result test machine

SAMPLE	**Test Results(Rockwell Hardness Values)**					
	T1	T2	T3	T4	T5	AVG
CHINA	117.5	119	119	117.5	118	118
ETH-L1	124	124	123.6	123.8	124	123.9
BRAZIL	124	124.5	124	124.5	124	124
MINTEX	69.5	70	70	71.5	70	70.2

- **Wear experiment and Chase Machine**

JF160 chasese taster

Use quality controlling and classing friction material to the standards
i.e SAE J661
ISO 7881
GB/T 17469-98

Characterstics

The taster is designed reffering to the theoery and based stracture of imported taster from standard of AMERICAN FF SAE J661 and combined modern technology.The posetive pressure is controlled by yhe haydrolic servo and has the controlling function of constant friction, the main parameters is confirmed for the developing of future testing standard. Control and data treat by th computer the machine is equipped with digital display torque,pressure, speed and temprature.The result and curve is printed out by printer.detail specifcation of SAE J661 machine in Appendix I B.

The friction tests were performed using the friction material test machine called CHASE machine. The CHASE used a pearlitic gray cast iron disc (diameter of 180 mm, thickness 38 mm) and a brake lining test sample with dimensions of 25 mm x 25 mm x 7 mm. The test sample was mounted on the load arm and 150 psi pressure was pressed against the flat surface of the rotating disc. The rotating cast iron disc moved with a constant sliding speed of 411 rpm.

The table 8 shows comparison test results of Awash Arba brake liner (ETH-L1) and commercial brake liners. The normal/ hot friction coefficient test results were summarized from average samples of AWABPAL and commercial brake liner formulation individually. The results demonstrated that the formulations using AWABPAL liner (ETH-L1) produced higher normal and hot friction coefficient at FF, EE and DE class value than those of the commercial brake pad samples.

Table 7 Summary of test results

Group of Brake liner	Normal friction coefficient	Hot friction coefficient
ETH-L1	0.426 F	0.366 F
BRAZIL	0.388 F	0.37 F
CHINA	0.249 D	0.281 E
MINTEX	0.28 E	0.265 E

✓ **First Baseline**

The Figure 23 shows the samples run for first base line condition. The load was applied to the drum for 10 seconds and released for 20 seconds for 20 applications with friction readings taken at every fifth application. The temperatures range from 92°C-101°C during the testing procedure. All the friction coefficient of samples increased at the beginning of braking stages until 20 braking applications. Among this sample Brazil liner showed the highest trend while Mintex liner was the lowest.

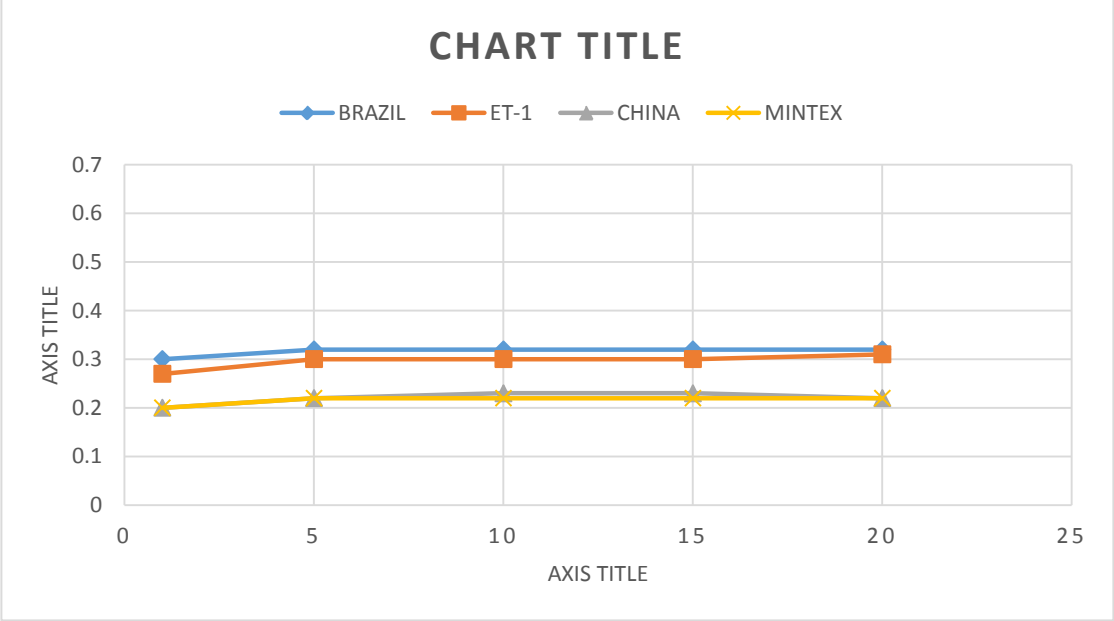

Figure 23 Plots of friction coefficient for first baseline condition

However the friction coefficient of commercial sample became low at the fifth application and eventually constant after 20 applications. Heat generated during braking caused the surface temperature to increase with braking time which resulting the creating of tribo-films. For the commercial brake pad, tribo films which were in the forms of Carbon started to create at the fifth application. The increase of tribo-films was accompanied by a decrease in friction coefficient at the fifth application onwards. The Figure 24 shows the changes of the friction coefficient as a function of disc temperature during the first fade condition for all samples. The load was applied continuously for 10 minutes or until the temperature reached 290ºC. The coefficient of friction was recorded with each increase in the temperature. Friction readings were taken at average of 28°C intervals.

✓ **First fade**

Fade it is the stage which is the temperature rise maximum and the critical braking condition happens.

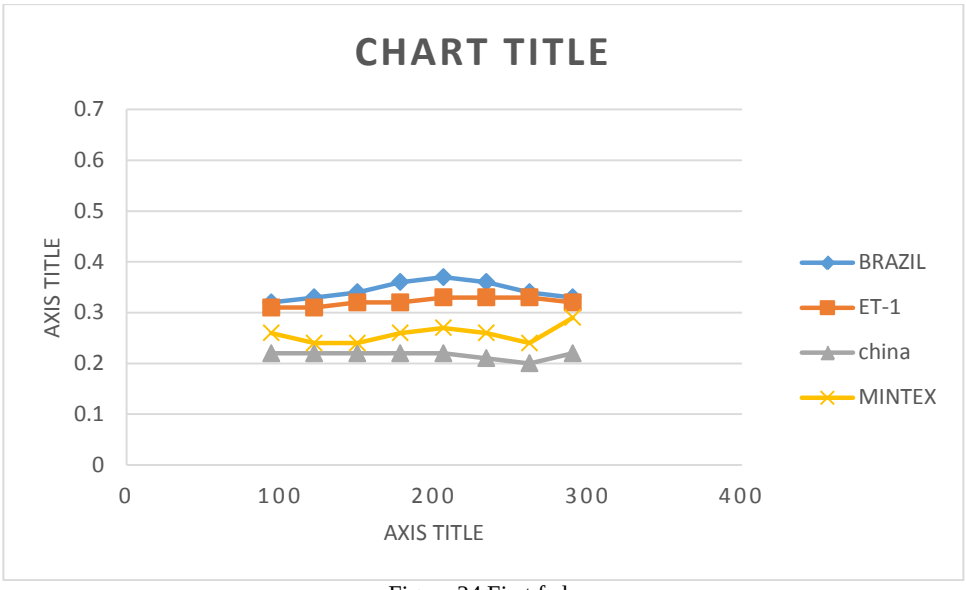

Figure 24 First fade

When the friction coefficient decreases during braking due to the friction heat, the situation is referred to as fade and it is caused by thermal decomposition of ingredients in the brake lining. The current study examined the changes of friction coefficient at temperatures of 101°C to 290°C. It appeared that an overall friction coefficient value declined with the increase in drum temperature. However the reduction of friction coefficient for all ETH-L1 brake pads was much more constant and stable as compared to the commercial brake pad.

- ✓ **First recovery condition**

Figure 4.225 shows friction coefficient during first recovery condition for all samples. During the recovery part of the test the drum was allowed to cool. The brake was applied and friction readings were taken at 54°C intervals. For the first recovery the drum temperature reduced from 262°C to 101°C.

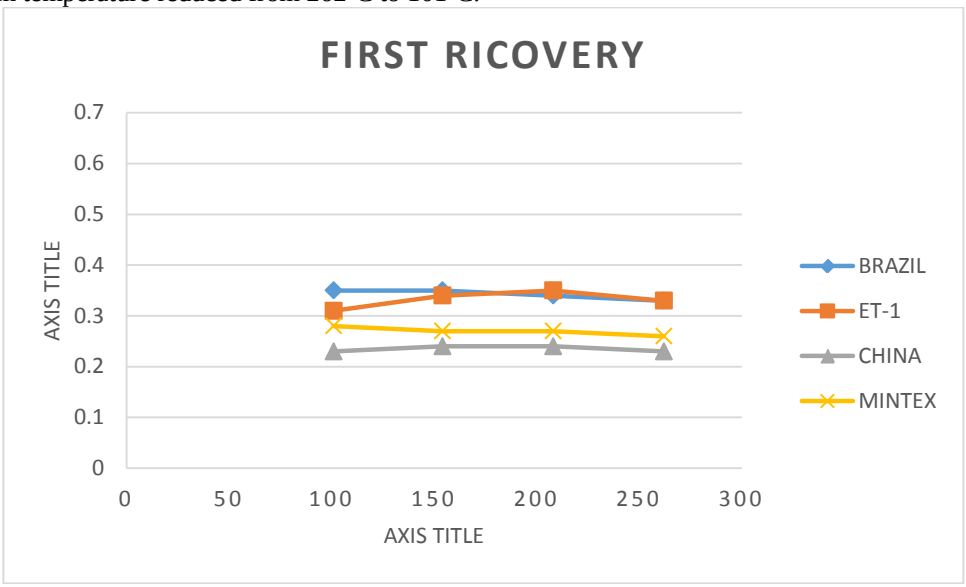

Figure 25 First recovery plots of friction coefficient

The significant difference of recovery phase was portrayed in the commercial brake pad sample where the friction coefficient increased from 0.23 to 0.24 at temperatures of 252°C to 92°C. However, for the ETH-L1 brake pad samples, the average friction coefficient decreased from 0.35 to 0.31 at the temperature of 262°C to 100°C temperatures. Friction fade took place at high temperature but recovered rapidly upon cooling. The most desired situation is normal recovery, which is when friction coefficient returns to its pre-fade friction level with a little temperature reduction. Therefore, the recovery

condition for both ET-1 and commercial brake pads were normal as they were able to return to its pre-fade friction coefficient level. Heat generated during braking caused the surface temperature to increase with braking time. During this experiment the onset of degradation of friction material started at 205°C.Therefore during the cooling stage the phenomenon of degradation was diminishing.

✓ **Wear test condition**

The Figure 4.26 reveals the graph of friction coefficient collected during wear test application. The load was applied for 20 seconds and released for 10 secondsfor100 applications.

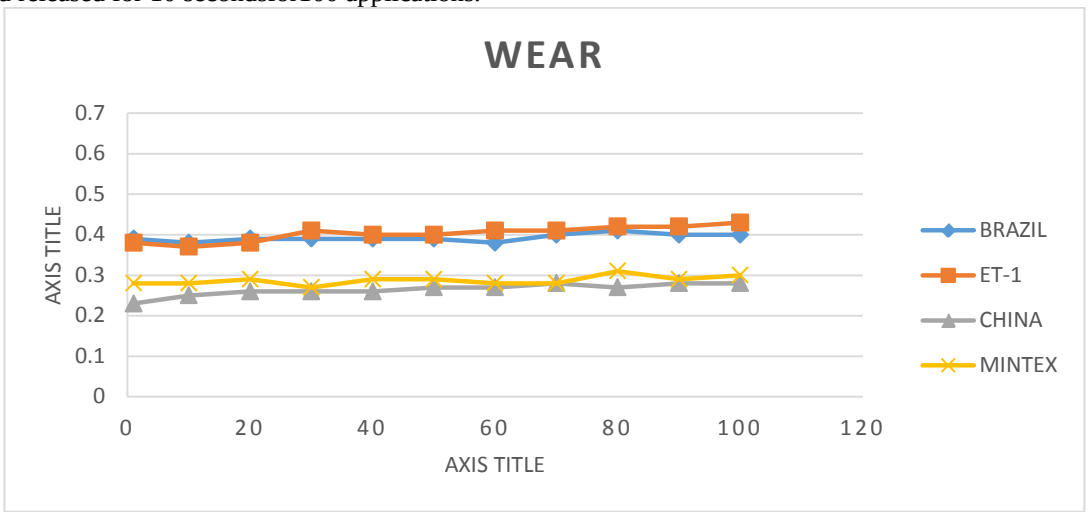

Figure 26 Plots of friction coefficient during wear test condition

The friction coefficient results showed a trend which is similar to the initial baseline result except for the condition of braking time that was prolonged until 100 applications. Friction coefficient value of Commercial sample significantly reduced. All samples show high and constant friction coefficient at the beginning of the braking stages caused by direct contacts of the brake pads and rotor surfaces without the formation of tribo-films.

✓ **Second fade condition**

The Figure 4.27 shows the friction coefficient behavior during the second fade condition. The load was applied continuously for 10 minutes or until 346°C. The coefficient was recorded with every increase of 28°C in the temperature. The friction coefficient value for commercial sample started to decrease from 0.37 at 262°C to 0.33 at 346°C.

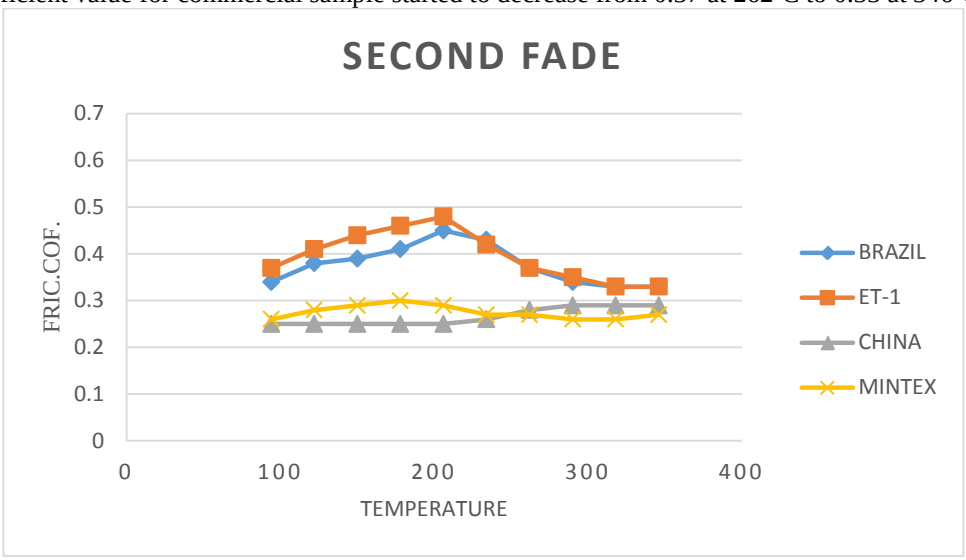

Figure 27 Plots of friction coefficient during second fade

✓ **Second recovery condition**

The Figure 28 shows friction coefficient during second recovery condition for all samples. During the recovery part of the test the drum was allowed to cool. The load was applied for 10 seconds at 54°C increments as the drum cools from 316°C

to 101°C. The graph also shows a trend similar to the first recovery condition. The significant different of recovery phase can be seen for the commercial brake pad sample where the friction coefficient shows an decreasing trend from 0.42 at 155^{o}C to 0.34 at 314^{o}C. Also for the mintex brake pad samples the average of friction coefficient decreased from 0.3 to 0.26 at 218^{0}C to 315^{0}Ctemperature range. Thus, both ET-1 and commercial brake pads showed normal recovery when they returned to their pre-fade friction coefficient level.

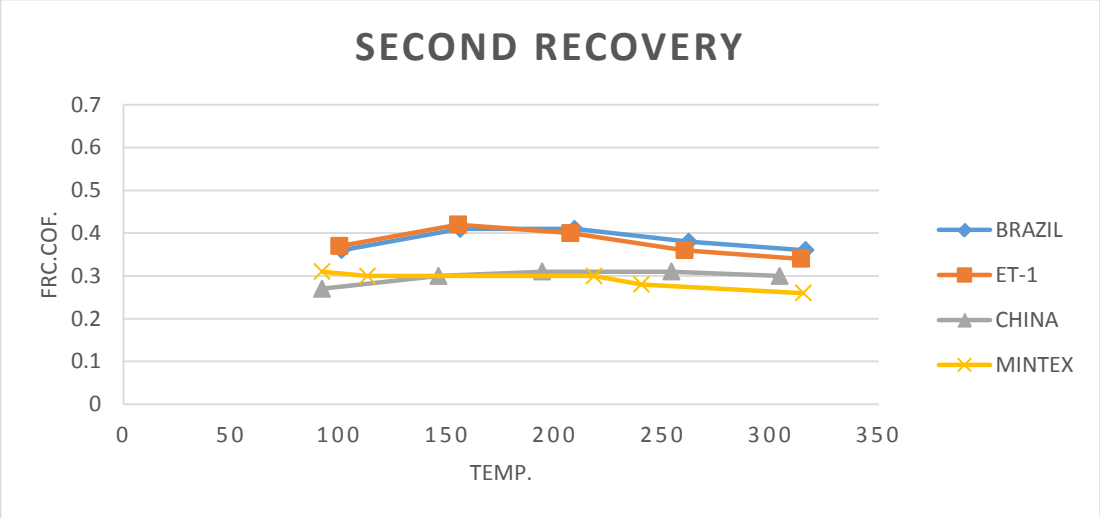

Figure 28 Plots of friction coefficient during second recovery

Final baseline condition

The Figure 4.29 shows friction coefficient during final baseline. The load was applied to the drum for 10 seconds and released for 20 seconds for 20 applications, with a drum temperature of 106°C to 86°C. The friction coefficient for all samples show trend similar to initial baseline condition. All ET-1 and commercial samples experienced decreases in friction coefficient at the beginning of the braking stages until 5 braking applications and continued constant. As explained in the initial base line stage, friction coefficient increased when direct contacts of the ingredients in the lining and rotor surfaces occur at the friction interface without tribo-films. It was also associated with the increase of the real area of contact during sliding stages.

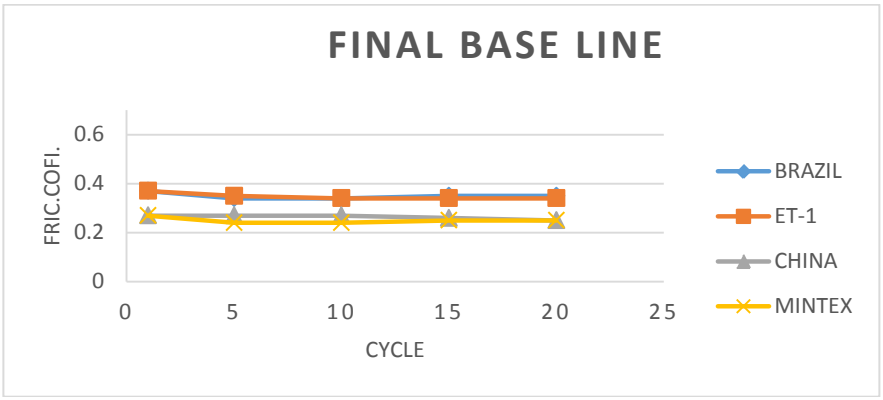

Figure 29 Plots of friction coefficient during second fade

5 Conclusions and Recommendations

In this thesis work, Finite Element analysis procedure developed to study mechanical and thermal analysis in drum brake and liner and also investigate experimentally the wear and hardness of different friction plate using chassis and rock well hardness test machine . This simulation results states the prediction of stress, displacement and of the two models by stimulating them with the brake shoe force of 4996N with the velocity of 60km/hr. during emergency braking. The minimum von mises stress and displacement are located at the adjacent side of the inner part of the two brake drum models. This is due to absence of forces acting directly on these surfaces. While the maximum von mises stress of the two models

are located on the walls of the brake drums. This is due to the action of the brake shoes on the brake drum. The finned brake drum model shows a lower value of stress and displacement than the normal model. This indicates that the fins have added more circumferential strength on the brake drum. This circumferential strength has increased the circumferential resistance of the brake drum to the action of the brake shoe force. This has also makes the brake drum to be more rigid. This helps to reduce hoop or circumferential stress acting at the inner wall of the brake drum. This circumferential stress is produce when the brake drum is under pressure by the action of the brake shoes during braking. The thermal analysis result shows that the lower value of temperature on finned drum brake more heat dissipate than the normal drum brake and analysis the other components of drum brake such as the brake liner and friction plate with the same loads.

The experimental study investigates the effect of wear and hardness on the friction plate based on the chassis and rock well hardness test machine. Friction coefficient of Ethiopian awash Arba brake friction plate (ET-1) brake fiction plate and commercial brake friction plate were significantly different. The average friction coefficient of all four ET-1 brake friction plate was 0.426 (0.038 higher than the sample of commercial brazil brake friction plate and 0.177 & 0.146 higher than China and Mintex sample of friction plates respectively).

The abrupt reduction of friction coefficient which is known as fade was more significant in the commercial brake friction plate samples than in ET-1 brake friction plate. Fade occurred in commercial brake friction plate sample at the lower temperature; i.e. the first fade was at 122^{o}C and the second was at 206^{o}C.ET-1 were more stable and constant than their commercial counterparts. For ET-1 brake pads, the study reported only a slight reduction of friction coefficient at a temperature of 262^{o}C during the first fade and 206^{o}C on the second. This was resulted from high thermal conductivity. And also checking the local Ethiopian friction plate by Jf 150 friction material waer test machine in constant speed at varation of temprature the result of wear rate shows that between the standard.

Appendix I

A. Brazil brake lining chase wear test report

ISSN (Online) 2348 – 7968
www.ijiset.com

Chase SAE J-661 Friction Material Test Report

Manufacturer: Brazile brake lining 4/28/2019
Material:
Test Pressure: 150 psi

Normal=	0.388	F
Hot=	0.370	F

Wear Data

	Start	Finish	Loss	%Loss
Weight(g)	7.13	6.87	0.26	3.65
Thick.(mm)	6.13	5.97	0.16	2.61

Baseline

	Initial		Final	
Application	Force(N)	μ	Force(N)	μ
1	198	0.301	245	0.37
5	209	0.317	226	0.343
10	211	0.32	227	0.343
15	211	0.32	230	0.348
20	212	0.321	231	0.349

Wear

Application	Force(N)	μ
1	188	0.39
10	254	0.384
20	258	0.392
30	259	0.393
40	255	0.387
50	260	0.393
60	254	0.385
70	261	0.396
80	269	0.408
90	264	0.4
100	262	0.397

First Fade

Application	Force(N)	μ	Temp.(℃)
1	212	0.322	94
2	220	0.333	122
3	225	0.34	150
4	236	0.357	178
5	242	0.367	206
6	239	0.363	234
7	223	0.339	262
8	216	0.326	290

Time: 5:28

Second Fade

Application	Force(N)	μ	Temp.(℃)
1	225	0.34	94
2	249	0.377	122
3	256	0.388	150
4	268	0.405	178
5	295	0.448	206
6	286	0.434	234
7	244	0.369	262
8	224	0.34	290
9	219	0.333	318
10	219	0.332	346

Time: 7:37

First Recovery

Application	Force(N)	μ	Temp.(℃)
1	220	0.333	262
2	228	0.345	208
3	231	0.35	154
4	229	0.347	101

Second Recovery

Application	Force(N)	μ	Temp.(℃)
1	237	0.359	316
2	250	0.379	262
3	269	0.408	209
4	269	0.406	156
5	240	0.362	101

IJISET - International Journal of Innovative Science, Engineering & Technology, Vol. 6 Issue 6, June 2019
ISSN (Online) 2348 – 7968
www.ijiset.com

Chase SAE J-661 Friction Material Test Report

Manufacturer: Brazil brake lining 4/28/2019
Material:
Test Pressure: 150 psi

Initial Baseline

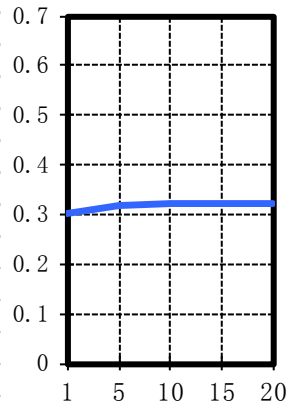

Wear Test

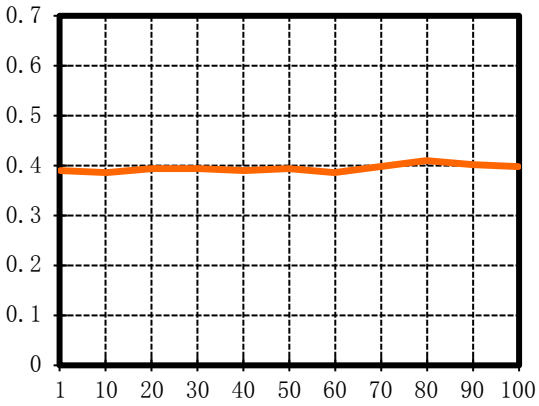

Final Baseline

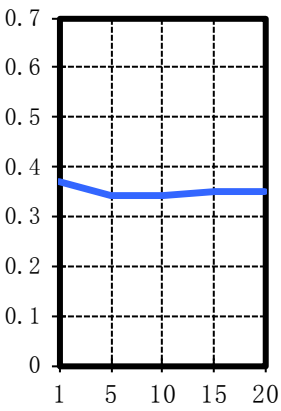

First Fade

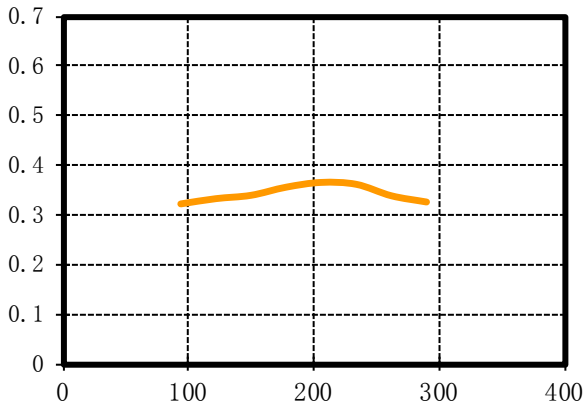

First Recovery

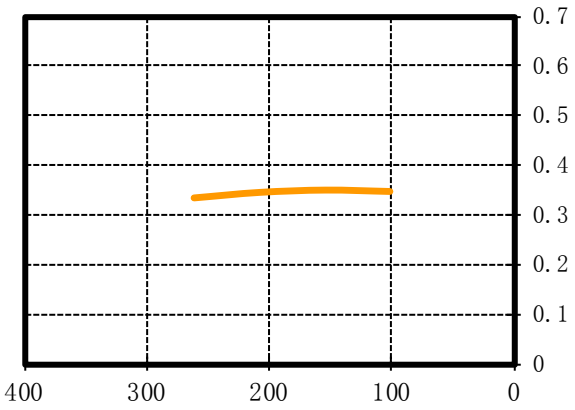

Second Fade

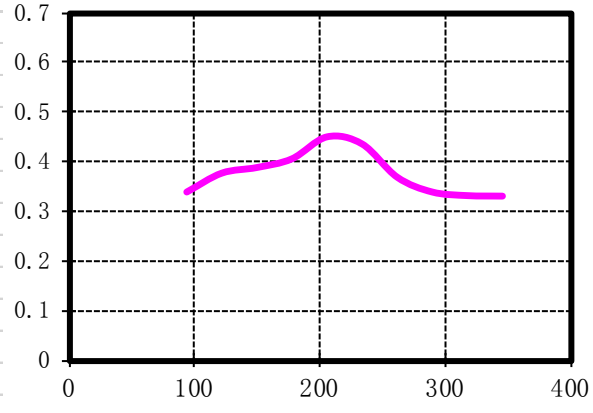

Second Recovery

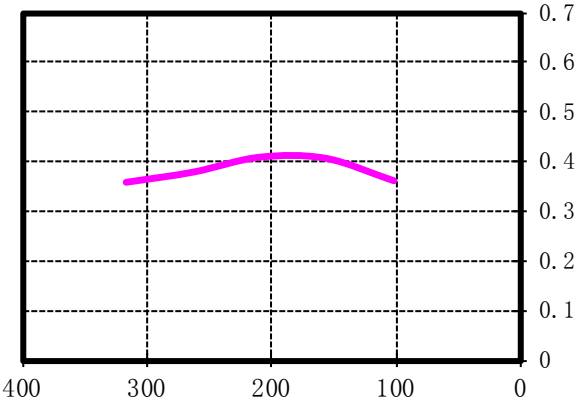

IJISET - International Journal of Innovative Science, Engineering & Technology, Vol. 6 Issue 6, June 2019
ISSN (Online) 2348 – 7968
www.ijiset.com

SAE J661Friction Material Test Report

Manufacturer	Brazil brake lining	Test NO.	
Material		Date	4/28/2019

Wear Data	Initial	Finial	Loss	%Loss
Weight(g)	7.13	6.87	0.26	3.6
Thickness(mm)	6.13	5.97	0.16	2.6

First Base Line
411r/min
150lib

CYCL	T(℃)	F(N)	μ
1	94	198	0.30
5	93	209	0.32
10	92	211	0.32
15	92	211	0.32
20	92	212	0.32

First Fade
411 r/min,150lib
heat to 288℃ in 10 min

T(℃)	F(N)	μ
94	212	0.32
122	220	0.33
150	225	0.34
178	236	0.36
206	242	0.37
234	239	0.36
262	223	0.34
290	216	0.33

Time: 328 s

First Recovery
150lb,408r/min

T(℃)	F(N)	μ
262	220	0.33
208	228	0.34
154	231	0.35
101	229	0.35

Classification

	μ	Class
Normal	0.388	F
Heat	0.370	F

Wear Test

CYCL	T(℃)	F(N)	μ
1	218	188	0.39
10	212	254	0.38
20	212	258	0.39
30	202	259	0.39
40	204	255	0.39
50	205	260	0.39
60	218	254	0.38
70	204	261	0.4
80	205	269	0.41
90	219	264	0.4
100	204	262	0.4

Second Base Line
411r/min
150lib

CYCL	T(℃)	F(N)	μ
1	106	245	0.37
5	91	226	0.34
10	92	227	0.34
15	93	230	0.35
20	92	231	0.35

Second Fade
411 r/min,150lib
heat to 343℃ in 10 min

T(℃)	F(N)	μ
94	225	0.34
122	249	0.38
150	256	0.39
178	268	0.41
206	295	0.45
234	286	0.43
262	244	0.37
290	224	0.34
318	219	0.33
346	219	0.33

Time: 458 s

Second Recovery
150lb,408r/min

T(℃)	F(N)	μ
316	237	0.36
262	250	0.38
209	269	0.41
156	269	0.41
101	240	0.36

B. ETH-L1 chase test report

Chase SAE J-661 Friction Material Test Report

Manufacturer: ETH-L1 3/20/2019
Material:
Test Pressure: 150 psi

Normal= 0.426 F
Hot= 0.366 F

Wear Data

	Start	Finish	Loss	%Loss
Weight(g)	6.36	6.26	0.1	1.57
Thick.(mm)	6	5.97	0.03	0.50

Baseline

	Initial		Final	
Application	Force(N)	μ	Force(N)	μ
1	178	0.27	241	0.365
5	198	0.301	231	0.351
10	200	0.302	227	0.344
15	200	0.304	227	0.344
20	204	0.309	227	0.345

Wear

Application	Force(N)	μ
1	249	0.377
10	243	0.37
20	254	0.385
30	269	0.407
40	263	0.398
50	265	0.401
60	271	0.409
70	270	0.409
80	275	0.418
90	277	0.419
100	282	0.427

First Fade

Application	Force(N)	μ	Temp.(℃)
1	205	0.311	94
2	207	0.313	122
3	211	0.319	150
4	215	0.325	178
5	216	0.327	206
6	220	0.334	234
7	218	0.331	262
8	209	0.316	290

Time: 5:39

Second Fade

Application	Force(N)	μ	Temp.(℃)
1	246	0.372	94
2	272	0.412	122
3	288	0.437	150
4	305	0.462	178
5	318	0.482	206
6	276	0.419	234
7	243	0.369	262
8	229	0.346	290
9	220	0.334	318
10	220	0.333	346

Time: 7:44

First Recovery

Application	Force(N)	μ	Temp.(℃)
1	217	0.329	262
2	229	0.347	208
3	222	0.337	154
4	207	0.314	100

Second Recovery

Application	Force(N)	μ	Temp.(℃)
1	228	0.345	314
2	236	0.357	260
3	266	0.403	207
4	277	0.419	155
5	247	0.374	100

ISSN (Online) 2348 – 7968
www.ijiset.com

Chase SAE J-661 Friction Material Test Report

Manufacturer: ETH-L1 3/20/2019
Material:
Test Pressure: 150 psi

Initial Baseline

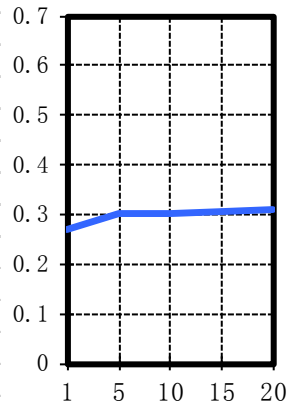

Wear Test

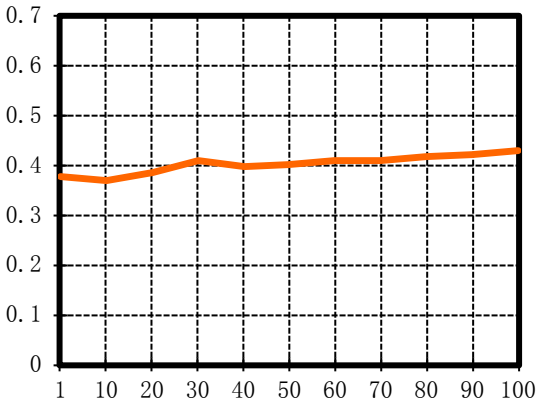

Final Baseline

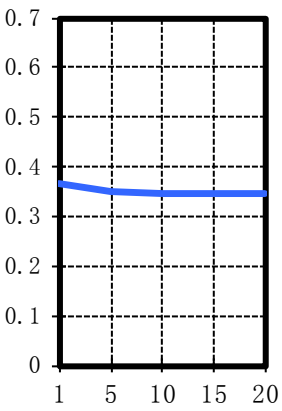

First Fade

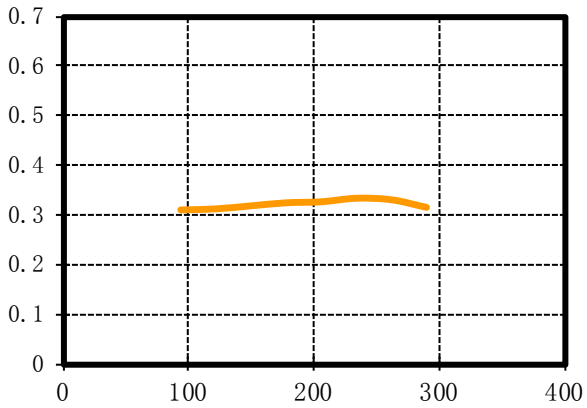

First Recovery

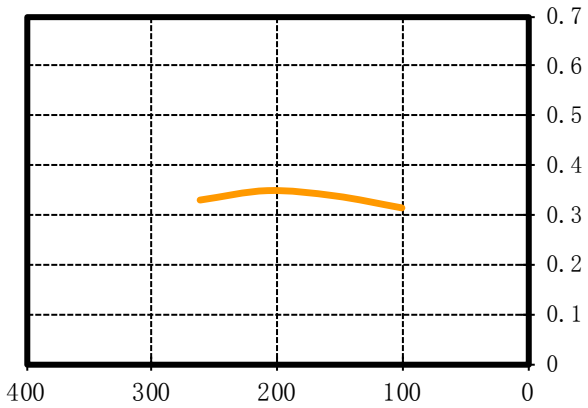

Second Fade

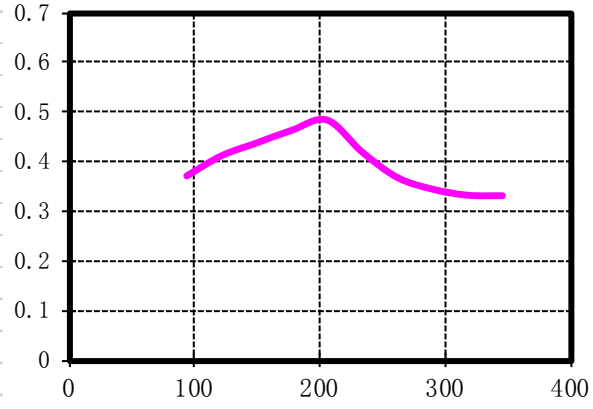

Second Recovery

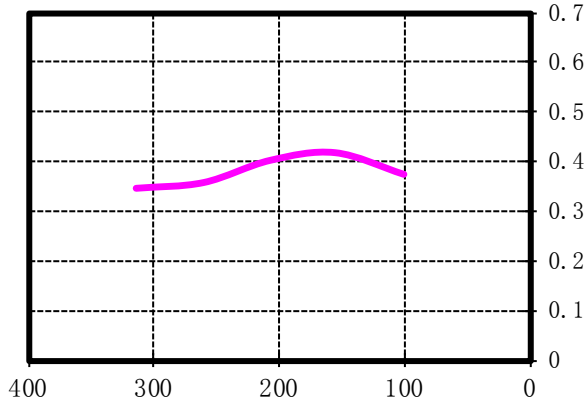

IJISET - International Journal of Innovative Science, Engineering & Technology, Vol. 6 Issue 6, June 2019
ISSN (Online) 2348 – 7968
www.ijiset.com

SAE J661Friction Material Test Report

Manufacturer	ETH-L1	Test NO.	
Material		Date	3/20/2019

Wear Data	Initial	Finial	Loss	%Loss
Weight(g)	6.36	6.26	0.10	1.6
Thickness(mm)	6	5.97	0.03	0.5

First Base Line
411r/min
150lib

CYCL	T(℃)	F(N)	μ
1	92	178	0.27
5	94	198	0.30
10	91	200	0.30
15	92	200	0.30
20	92	204	0.31

First Fade
411 r/min,150lib
heat to 288℃ in 10 min

T(℃)	F(N)	μ
94	205	0.31
122	207	0.31
150	211	0.32
178	215	0.32
206	216	0.33
234	220	0.33
262	218	0.33
290	209	0.32

Time: 339 s

First Recovery
150lb,408r/min

T(℃)	F(N)	μ
262	217	0.33
208	229	0.35
154	222	0.34
100	207	0.31

Classification

	μ	Class
Normal	0.426	F
Heat	0.366	F

Wear Test

CYCL	T(℃)	F(N)	μ
1	221	249	0.38
10	211	243	0.37
20	211	254	0.38
30	200	269	0.41
40	211	263	0.4
50	211	265	0.4
60	200	271	0.41
70	212	270	0.41
80	211	275	0.42
90	200	277	0.42
100	213	282	0.43

Second Base Line
411r/min
150lib

CYCL	T(℃)	F(N)	μ
1	92	241	0.37
5	93	231	0.35
10	91	227	0.34
15	92	227	0.34
20	91	227	0.34

Second Fade
411 r/min,150lib
heat to 343℃ in 10 min

T(℃)	F(N)	μ
94	246	0.37
122	272	0.41
150	288	0.44
178	305	0.46
206	318	0.48
234	276	0.42
262	243	0.37
290	229	0.35
318	220	0.33
346	220	0.33

Time: 464 s

Second Recovery
150lb,408r/min

T(℃)	F(N)	μ
314	228	0.34
260	236	0.36
207	266	0.4
155	277	0.42
100	247	0.37

C. China brake lining chase test report

Chase SAE J-661 Friction Material Test Report

Manufacturer: China Brake Lining 4/29/2019
Material: AA 1
Test Pressure: 150 psi

Normal= 0.249 D
Hot= 0.281 E

Wear Data

	Start	Finish	Loss	%Loss
Weight(g)	7.65	7.21	0.44	5.75
Thick.(mm)	6.14	5.92	0.22	3.58

Baseline

	Initial		Final	
Application	Force(N)	μ	Force(N)	μ
1	130	0.197	179	0.271
5	142	0.215	180	0.273
10	151	0.228	177	0.269
15	151	0.229	171	0.26
20	147	0.223	167	0.253

Wear

Application	Force(N)	μ
1	151	0.229
10	163	0.246
20	170	0.257
30	172	0.26
40	175	0.265
50	176	0.267
60	176	0.267
70	181	0.275
80	180	0.273
90	182	0.276
100	182	0.276

First Fade

Application	Force(N)	μ	Temp.(℃)
1	144	0.218	94
2	147	0.222	122
3	146	0.222	150
4	145	0.22	178
5	142	0.216	206
6	137	0.208	234
7	133	0.201	262
8	144	0.218	290

Time: 8:39

Second Fade

Application	Force(N)	μ	Temp.(℃)
1	164	0.248	94
2	166	0.251	122
3	165	0.25	150
4	162	0.245	178
5	164	0.248	207
6	171	0.26	234
7	183	0.278	262
8	192	0.292	290
9	193	0.292	318
10	189	0.289	332

Time: 10:02

First Recovery

Application	Force(N)	μ	Temp.(℃)
1	152	0.23	252
2	159	0.24	200
3	156	0.237	143
4	151	0.229	92

Second Recovery

Application	Force(N)	μ	Temp.(℃)
1	195	0.296	304
2	203	0.308	254
3	206	0.312	194
4	197	0.298	146
5	179	0.271	92

ISSN (Online) 2348 – 7968
www.ijiset.com

Chase SAE J-661 Friction Material Test Report

Manufacturer:	China Brake Lining	4/29/2019
Material:	AA	1

Test Pressure: 150 psi

Initial Baseline

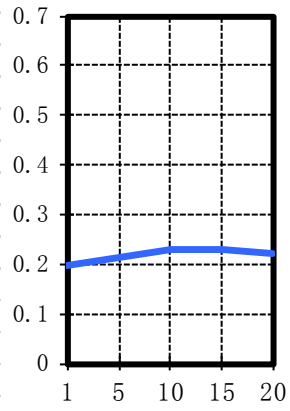

Wear Test

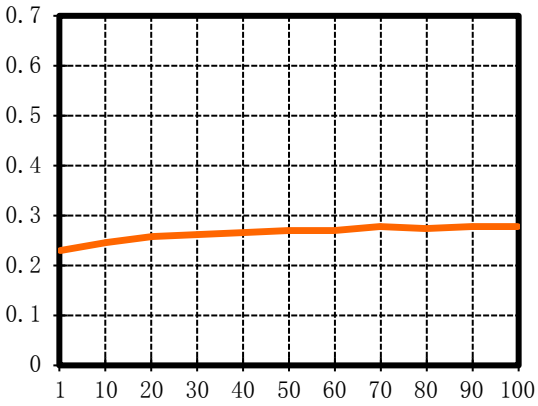

Final Baseline

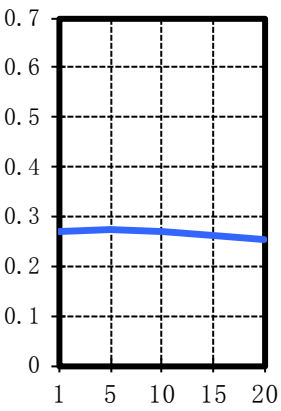

First Fade

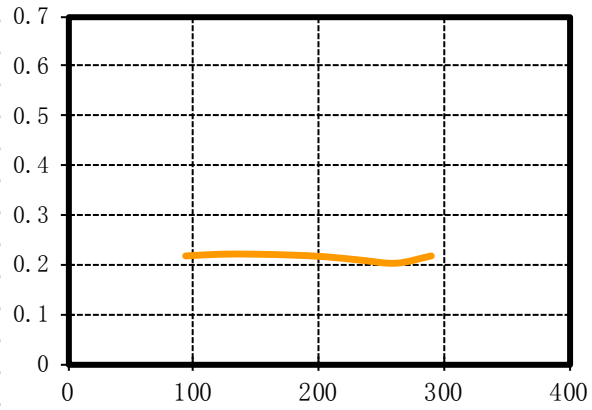

First Recovery

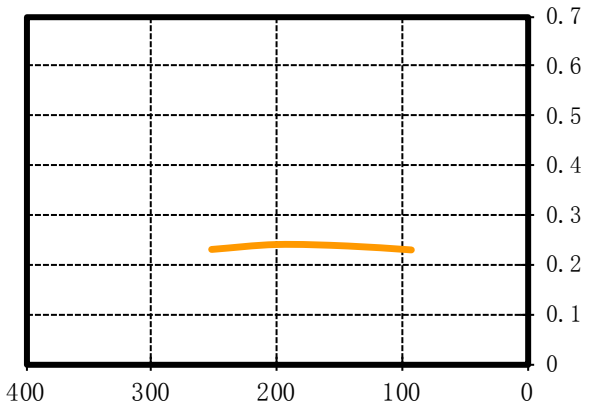

Second Fade

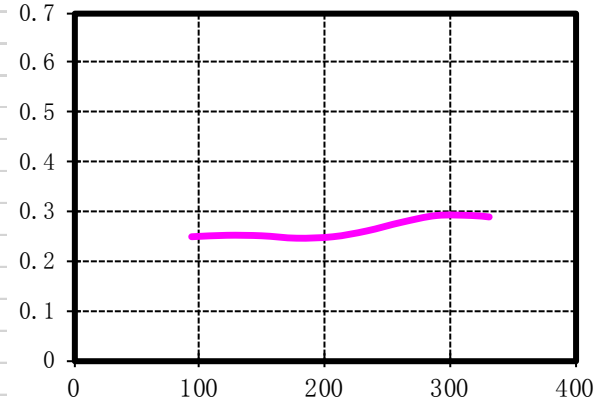

Second Recovery

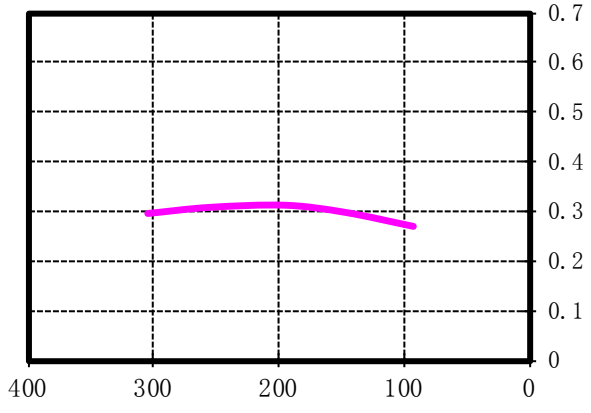

IJISET - International Journal of Innovative Science, Engineering & Technology, Vol. 6 Issue 6, June 2019
ISSN (Online) 2348 – 7968
www.ijiset.com

SAE J661Friction Material Test Report

Manufacturer	China Brake Lining	Test NO.	1
Material	AA	Date	4/29/2019

Wear Data	Initial	Finial	Loss	%Loss
Weight(g)	7.65	7.21	0.44	5.8
Thickness(mm)	6.14	5.92	0.22	3.6

First Base Line
411r/min
150lib

CYCL	T(℃)	F(N)	μ
1	82	130	0.20
5	87	142	0.22
10	86	151	0.23
15	89	151	0.23
20	90	147	0.22

First Fade
411 r/min,150lib
heat to 288℃ in 10 min

T(℃)	F(N)	μ
94	144	0.22
122	147	0.22
150	146	0.22
178	145	0.22
206	142	0.22
234	137	0.21
262	133	0.20
290	144	0.22

Time: 519 s

First Recovery
150lb,408r/min

T(℃)	F(N)	μ
252	152	0.23
200	159	0.24
143	156	0.24
92	151	0.23

Classification

	μ	Class
Normal	0.249	D
Heat	0.281	E

Wear Test

CYCL	T(℃)	F(N)	μ
1	203	151	0.23
10	211	163	0.25
20	199	170	0.26
30	210	172	0.26
40	200	175	0.26
50	198	176	0.27
60	210	176	0.27
70	206	181	0.28
80	199	180	0.27
90	210	182	0.28
100	212	182	0.28

Second Base Line
411r/min
150lib

CYCL	T(℃)	F(N)	μ
1	90	179	0.27
5	90	180	0.27
10	90	177	0.27
15	86	171	0.26
20	86	167	0.25

Second Fade
411 r/min,150lib
heat to 343℃ in 10 min

T(℃)	F(N)	μ
94	164	0.25
122	166	0.25
150	165	0.25
178	162	0.25
207	164	0.25
234	171	0.26
262	183	0.28
290	192	0.29
318	193	0.29
332	189	0.29

Time: 602 s

Second Recovery
150lb,408r/min

T(℃)	F(N)	μ
304	195	0.3
254	203	0.31
194	206	0.31
146	197	0.3
92	179	0.27

D. Mintex brake lining chase test report

SAE J661Friction Material Test Report

Manufacturer	Mintex Brake Lining	Test NO.	
Material		Date	3/19/2019

Wear Data	Initial	Finial	Loss	%Loss
Weight(g)	6.11	5.89	0.22	3.6
Thickness(mm)	6.04	5.78	0.26	4.3

First Base Line
411r/min
150lib

CYCL	T(℃)	F(N)	μ
1	94	198	0.2
5	93	208	0.22
10	92	208	0.22
15	92	211	0.22
20	92	212	0.22

First Fade
411 r/min,150lib
heat to 288℃ in 10 min

T(℃)	F(N)	μ
92	212	0.26
125	220	0.24
155	225	0.24
175	236	0.26
206	242	0.27
235	239	0.26
252	223	0.24
280	216	0.29

Time: 328 s

First Recovery
150lb,408r/min

T(℃)	F(N)	μ
232	220	0.26
248	228	0.27
154	231	0.27
101	229	0.28

Classification

	μ	Class
Normal	0.28	E
Heat	0.265	E

Wear Test

CYCL	T(℃)	F(N)	μ
1	213	148	0.28
10	211	234	0.28
20	210	234	0.29
30	210	255	0.27
40	204	255	0.29
50	205	260	0.29
60	205	254	0.28
70	204	261	0.28
80	205	269	0.31
90	219	264	0.29
100	204	262	0.3

Second Base Line
411r/min
150lib

CYCL	T(℃)	F(N)	μ
1	106	245	0.27
5	94	226	0.24
10	91	227	0.24
15	91	230	0.25
20	92	231	0.25

Second Fade
411 r/min,150lib
heat to 343℃ in 10 min

T(℃)	F(N)	μ
94	225	0.26
123	249	0.28
123	249	0.29
178	268	0.3
178	295	0.29
234	295	0.27
252	244	0.27
290	224	0.26
318	224	0.26
346	219	0.27

Time: 458 s

Second Recovery
150lb,408r/min

T(℃)	F(N)	μ
215	227	0.26
220	227	0.28
218	269	0.3
113	269	0.3
92	230	0.31

E. Mesh independence of finned and normal drum brake

Normal drum brake Node Vs Stress	
Node	stress(N/m^2)
38953	2268000
70219	1881000
209272	1920000
452969	1993000
727857	1990000
1334685	1999000
3162201	2.05E+06

Finned drum brake Node Vs Stress	
Total nodes	stress
37876	2243701
61820	2057268
162361	2205616
331780	2205616
496575	2215881
958099	2215441
2089844	2184492

F. Spesfication Rock well hardness test machine

Spesfication Rock well hardness		
Inertia test force	N	98
Total test force	N	588,980,1471
Total test force keeping time	S	0-30
Test sample allowable max height	Mm	170
Distance of pressing head center and machine	Mm	165
Outside size	Mm	510×212×750
Hardness weight	Kg	85
Hardnes value range		HRE 70~94 HRL 100~120 HRM85~110 HRR114~125

G. Vehicle Liner and Drum specification for TOYOTA HIACE I wagon

Figure 30Toyota Hiace Wagon specification

Table 8 A, Toyota Hiace specification B, drum Brake specification C, brake Shoe specification

Toyota Hiace Specification		**Drum brake specification**		**Brake shoe specification**	
A		B		C	
Engine type	2.5D-4D(2KD HI)	Fitting position	Rear axle	Fitting position	Rear axle
Number of cylinder	4 in line	Br. drum outer diameter (mm)	272	Diameter (mm)	254
Transmission		Inner Brake Diameter	66.5	Width (mm)	52

		(mm)			
Gear box	4 A/T	Bolt hole circle ø(mm)	20		
Performance		Total Br. Drum Height (mm)	78		
Maximum speed (km/hr)	145	Max. skimmed drum measure (mm)	255.5		
Chassis		Weight (kg)	7		
Suspension type –front	Double wishbone, torsion bar spring with establisher bar	**Note:** to take the same specification for both type of drum brake			
suspension type –rear	semi trailing arm, coil spring				
Number of doors	4				
Load capacity					
Gross vehicle weight (kg)	1800				

Acknowledgment

I am gratefully acknowledges the help of my Advisor Maj. Dr. Bisrat Yoseph, who was always ready to give advice and who gave an encouragement to work and finish on this area. I want to express grateful thanks to AWASH ARBA BRAKE PAD FACTORY Administrator special thanks to laboratory crew lieutenant Nebiyu, Capitan Yonas and Ananya helps during this work.

References

[1] D. Ć. J. G. J. M. S. Veličković, "Analysis of Failure Causes and the Criticality Degree of Elements of Motor Vehicle's Drum Brakes," *Research Gate,* vol. 36, p. 12, 2014.

[2] "DESIGN AND ANALYSIS OF DRUM BRAKES," vol. 6, no. 1, 2017.

[3] "Structural and Thermal Analysis of Brake Drum," vol. 20, no. 8, 2014.

[4] "Thermal Analysis of a Rear Drum Brake for Lightweight Passenger Vehicles," 2014.

[5] X. W. Z. F. L. G. Ehtisham Shahid1, "Numerical Simulation of the Stress, Temperature & Wear Behaviours of the Drum Brake," China, 2018.

[6] AUTOMOTIVE LABORATORY MANUAL, Istanbul: Özgen AKALIN ,O. Akın KUTLAR.

[7] An Introduction to Modern Vehicle Design, Julian Happian-Smith.

[8] Shigley's Mechanical Engineering Design.

[9] U. A. P. O. Y. ,. M. B. N. Bako Sunday, "Development and Analysis of Finned Brake Drum Model Using Solidworks Simulation," vol. 4, no. 5, 2015.

[10] J. P. Holman, Heat Transfer, 4th Ed., McGraw-Hill , 1976.

[11] "A study of the wear mechanisms of disk and shoe brake pads," 2015.

[12] "DEVELOPMENT OF FRICTION PAD AND STUDY OF ITS WEAR CHARACTERISTICS," vol. 5, no. 2, 2017.

[13] "EXPERIMENTAL INVESTIGATION OF DRUM BRAKE PERFORMANCE FOR PASSENGER CAR," vol. 2, no. 12, 2014.

[14] "Friction Material Temperature Distribution and Thermal and Mechanical Contact Stress Analysis," 2014.

[15] "Structural Analysis of Dual Brake System," vol. 20, 2016.

[16] K. S. K. O. H. R. C. Hohmann*, "Contact analysis for drum brakes and disk brakes using ADINA," 1999.

[17] M. D. a. &. H. K. a. Khairul Fuad a, "TEMPERATURE AND THERMAL STRESSES IN A BRAKE DRUM SUBJECTED TO CYCLIC HEATING," 2015.

[18] H.-G. C. Dongyub Han, "Developing Sustainable New Drum Brake System through Life Cycle Assessment: A Case of US Trucks," vol. 1, no. 5, December - 2014.

[19] O. Martin, "Development of a Methodology for Design and Optimization of Multi-Material Objects for enhanced Thermal Behavior," March 10, 2004.

[20] Z. J. Zheng Bin, "Modal Analysis of the Brake Drum of Heavy-scale Automobile," 2017.

[21] Z. J. MAXun, "Numerical Simulation and Analysis for Transient Thermal Field of a Drum Brake Based on the Test," Shiyan City, Hubei Province, PR C, 2010.